Energy Reports 9 (2023) 5826–5842

Contents lists available at ScienceDirect

Energy Reports

journal homepage: www.elsevier.com/locate/egyr

Research paper

Design and performance analysis of hybrid MPPT controllers for fuel cell fed DC-DC converter systems

Shaik Rafikiran [a], G. Devadasu [b], C.H. Hussaian Basha [c], Pretty Mary Tom [c], Prashanth V. [c], Dhanamjayulu C. [d,*], Abhishek Kumbhar [c], S.M. Muyeen [e,*]

[a] Sri Venkateswara College of Engineering (Autonomous), Tirupati, AP, India
[b] CMR College of Engineering & Technology (Autonomous), Hyderabad, India
[c] EV R&D Laboratory, NITTE Meenakshi Institute of Technology, Bengaluru, India
[d] School of Electrical Engineering, Vellore Institute of Technology, Vellore, Tamilnadu, India
[e] Department of Electrical Engineering, Qatar University, Doha, 2713, Qatar

ARTICLE INFO

Article history:
Received 30 January 2023
Received in revised form 1 May 2023
Accepted 10 May 2023
Available online 21 May 2023

Keywords:
Convergence speed
DC-DC converter
Fuzzy controller
High voltage conversion ratio
Low steady-state fluctuations of MPP
Less voltage stress

ABSTRACT

Fuel cell-based power generation is the most utilized renewable energy source in the automotive industry because of its features clean energy, and less environmental pollution. The fuel cell output power is mainly depending on the operating temperature of the fuel cell. The fuel cell gives nonlinear voltage versus current characteristics. As a result, the extraction of maximum power from the fuel stack is very difficult. In order to extract the peak power from the fuel cell, a Maximum Power Point Tracking (MPPT) controller is used at various working temperature conditions of the fuel cell. The main contribution of this study is the introduction and comparative performance analysis of different hybrid MPPT controllers for selecting the optimum duty cycle for the fuel cell-fed boost converter system. The studied MPPT controllers are Adaptive Adjustable Step-based Perturb and Observe (AAS-P&O) controllers, Variable Step Value-Radial Basis Function Controller (VSV-RBFC), Adaptive Step Hill Climb (ASHC) based fuzzy technique, Variable P&O with Particle Swarm Optimization (VP&O-PSO), and Variable Step Grey Wolf Algorithm (VSGWA) based fuzzy logic controller. These hybrid MPPT controllers' comparative performance analysis has been done in terms of tracking speed of MPP, oscillations across MPP, design complexity of controller, ability to handle fast changes of temperature values, and accuracy of MPP tracking. From the simulative performance results, it is identified that the VSGWA-based fuzzy controller gives superior performance when compared to the other controllers.

© 2023 The Author(s). Published by Elsevier Ltd. This is an open access article under the CC BY license (http://creativecommons.org/licenses/by/4.0/).

1. Introduction

With global warming and the limited availability of non-renewable energy sources, all over the world focusing on renewable energy sources. In India, the central government is providing subsidies for the installation of renewable power generation systems in order to improve the availability of electrical power supply. The features of renewable energy sources are less pollution, high environmentally friendly, more flexibility, highly robust, and low implementation cost when compared to non-renewable sources (Zheng et al., 2023). In article Izdebski and Kosiorek (2023), the authors studied the installation cost and power generation expenses of renewable power generation systems. Based on that, the authors say that renewable power systems are giving more economic benefits when compared to non-renewable energy sources. However, renewable power generation systems consist of stochastic behavior at various peak load demand conditions (Guo and Sepanta, 2021). Also, the different energy storage constraints and the size of the battery are very crucial factors for the establishment of high-rated renewable power generation systems. So, most of the power generation industries are focusing on hydrogen energy-based power generation systems instead of solar, wind, and tidal power systems (Rasheed et al., 2022).

In the article Nayak et al. (2023), the authors utilized hydrogen as a fuel input to the PEMFC-fed induction motor system for supplying continuous power to the motor. From the literature survey, the fuel cells are classified as Alkaline Fuel Cells (AFC), Proton Exchange Membrane Fuel Cells (PEMFC), Direct Methanol Fuel Cells (DMFC), Reversible Model Fuel Cells (RMFC), Phosphoric Acid Fuel Cells (PAFC), and Molten Carbonate Fuel Cell (Yu et al., 2022). The AFC can also be called a bacon fuel cell, and it absorbs pure oxygen, and hydrogen in order to produce heat, electricity,

* Corresponding authors.
E-mail addresses: dhanamjayulu.c@vit.ac.in (Dhanamjayulu C.), sm.muyeen@qu.edu.qa (S.M. Muyeen).

https://doi.org/10.1016/j.egyr.2023.05.030
2352-4847/© 2023 The Author(s). Published by Elsevier Ltd. This is an open access article under the CC BY license (http://creativecommons.org/licenses/by/4.0/).

Nomenclature

MPPT	Maximum Power Point Tracking
AAS-P&O	Adaptive Adjustable Step-Perturb and Observe
VSV-RBFC	Variable Step Value-Radial Basis Function Controller
ASHC	Adaptive Step Hill Climb
VP&O-PSO	Variable Perturb & Observe-Particle Swarm Optimization
VSGWA	Variable Step Grey Wolf Algorithm
AFC	Alkaline Fuel Cells
PEMFC	Proton Exchange Membrane Fuel Cell
DMFC	Direct Methanol Fuel Cells
RMFC	Reversible Model Fuel Cell
PAFC	Phosphoric Acid Fuel Cell
MCFC	Molten Carbonate Fuel Cell
SOFS	Solid Oxide Fuel Stack
EV	Electric Vehicle
BG with FLC	Bond Graph with Fuzzy Logic Controller
Improved Beta with FLC	Improved beta value with Fuzzy Logic Controller
ICA with ANN	Imperialist Competitive Algorithm with Artificial Neural Network
MFSO with FLC	Modified Fluid Search Optimization with Fuzzy Logic Controller
RBF with FLC	Radial Basis Functional with Fuzzy Logic Controller
MMRF with FLC	Manta Ray Foraging Optimization with Fuzzy Logic Controller

and water. In this AFC, the redox reaction has happened between the oxygen and hydrogen. In this AFC, the electrodes are separated by using the porous matrix aqueous chemical (Yu et al., 2021). The features of this fuel stack are less sensitive to the impurity of supply fuels, high power density, high temperature withstand capability, and high efficiency when compared to the Solid Oxide Fuel Stack (SOFS). The disadvantage of this alkaline fuel cell is easily poisoned by absorbing carbon dioxide. Also, the cost of the purifier is very high.

In article Gong et al. (2022), the authors studied the SOFS at various water membrane conditions. In this SOFS, the ceramic electrolyte is interfaced in between the cathode, and anode for the electro chemical oxidization. The SOFS features are less operating cost, high input fuel flexibility, high working temperature capability which is nearly equal to the 1000 °C, and high stability (Promsen et al., 2022). Also, it gives less harmful gas emissions. However, the drawbacks of this SOFS are high start-up time and high chemical compatibility issues. So, the demerits of SOFS are limited by using the PAFS. The operating temperature capability of this fuel cell is 210 °C which is applied for commercial medium power applications (Wilailak et al., 2021). Here, the liquid phosphoric acid is used as an electrolyte. The advantages of PAFS are high-temperature stability, low installation cost, and attractive performance (Lu et al., 2019). As a result, the PAFS is utilized in early stationary applications. But this fuel cell is very less sensitive to carbon monoxide chemical substances.

In the article Szczśniak et al. (2020), the authors focused on Molten Carbonate Fuel Stack (MCFS) which is running at above 600 °C temperature. This fuel stack is used in military and industrial power supply applications. Here, the molten carbonate salt mixture act as an electrolyte, and non-precious metals are

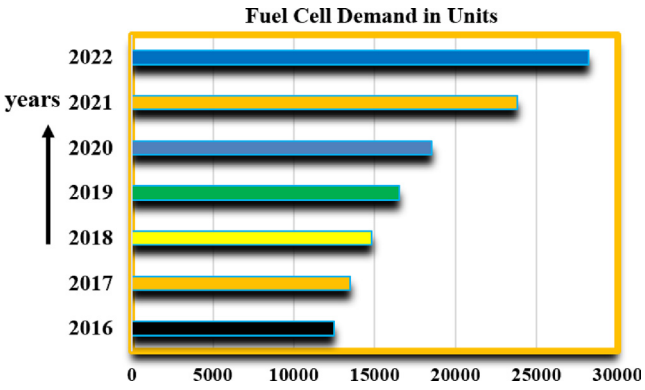

Fig. 1. Current statistics of fuel cell demand in units, (Alias et al., 2020).

applied as a catalyst at the cathode and anode of the fuel cell. So, the manufacturing cost of MCFS is less. Another factor of this fuel stack is high efficiency (Ferguson and Tarrant, 2021). As a result, an additional reformer is not required for the chemical energy transformation of the fuel cell. The drawbacks of MCFS are large space for mounting the fuel cell, less life span, and high carbon dioxide pollution. In article (Alias et al., 2020), the authors considered the DMFC and its working temperature is in between 70 °C to 130 °C. This type of fuel stack is used in mobile phones and portable devices. The chemical substance used in this stack is methanol. The methanol fuel stack features are easy transportation, and stable liquid under all environmental conditions. However, the disadvantages of the DMFC are high polarization of the anode, complex system design, and carbon monoxide poisoning. The demand for fuel cell units for every year in the current market is given in Fig. 1.

To limit the drawbacks of the above fuel stack technologies, in this work, a Proton Exchange Membrane Fuel Stack (PEMFS) is used for improving the power delivery capacity of the system with high operating efficiency. The advantages of PEMFS are less weight, fast start-up, low volume, high running speed, and high flexibility. The drawback of PEMFS is its nonlinear voltage versus current characteristics. So, the maximum power extraction from the fuel cell is very difficult. The MPPT controller is used in article Reddy et al. (2018) for enhancing the energy extraction of the fuel stack. From the literature review, the MPPT controllers are developed by utilizing the different types of soft computing, conventional, metaheuristic, and artificial neural network algorithms (Basha et al., 2022). From the previously available articles, the conventional MPPT techniques are used at static, and dynamic temperature conditions of the fuel cell. The P&O controller is one of the most utilized conventional MPPT controllers which is interfaced in the middle of the fuel cell, and load (Ge et al., 2015).

In this P&O method, the equivalent resistance of the fuel cell is adjusted in order to move the operating point of the fuel cell system at the required MPP position. Here, at an instant, the obtained fuel cell voltage is equated with the previously evaluated voltage value. The equated evaluation result gives a positive sign then the variation of step size is going to be in the same way. Or else, it moves opposite direction (Jayalakshmi et al., 2016). The merits of this controller are simplicity in design, easy understanding, less power consumption, plus good static response. However, the demerits of the P&O controller are fluctuations of MPP position, slow searching speed, and less accuracy for dynamic working temperature conditions (Somaiah and Agarwal, 2016). However, the drawbacks of conventional power point tracking controllers are limited by using the hybrid MPPT controller as shown in Fig. 2. The improved GWA-based fuzzy controller is shown in Fig. 2. The merits of this hybrid MPPT controller are fast MPP tracing speed

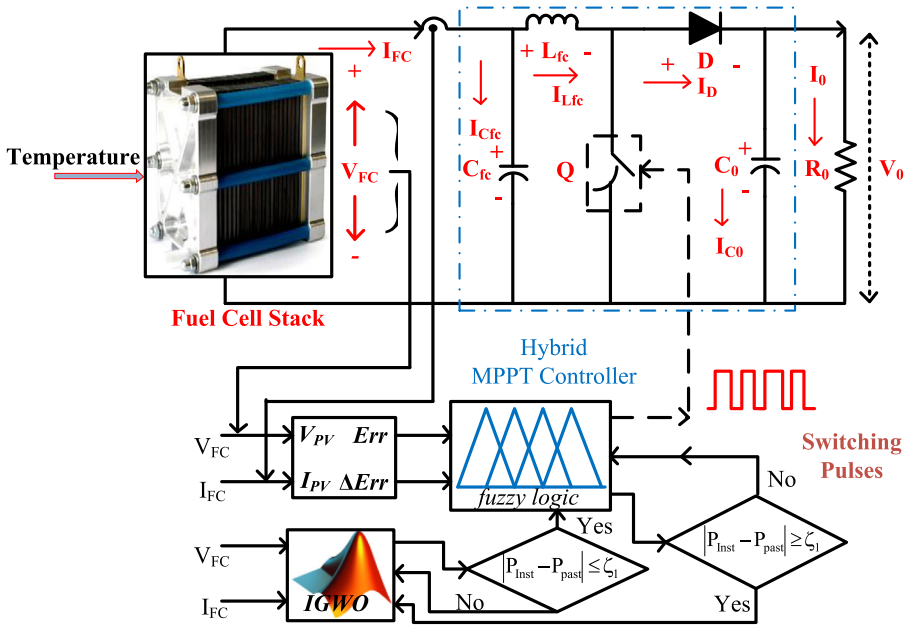

Fig. 2. Proposed power point tracking controller interfaced fuel cell system.

at both static, and dynamic operating temperature conditions, acceptable MPP tracking accuracy, low oscillations of fuel cell output voltage, and easy understanding. From Fig. 2, the fuel stack supplies a high current which is not useful for automotive industry applications. To improve the voltage profile of the fuel stack, a DC-DC power converter is interfaced in the middle of the supply, and resistive load.

As of now, the converters are classified as isolated, and transformerless DC-DC converters (Subhransu et al., 2016). The isolated converters needed an extra transformer, and rectifier for improving the voltage profile of the system. The isolated converter divides the entire circuit into two parts which are the source side electrical circuit, and the load side power supply. These two parts are separated physically to make the working circuit in a safe zone from the higher fluctuated supply voltages (Tytelmaier et al., 2016). Here, the DC-path is eliminated in between the supply, and load. The features of the isolated converters are high implementation size, more cost for design, high power losses, high safety needed, ground-breaking loops, limited applications, and moderate efficiency. In article Hwu et al. (2016), the authors explained the isolated methodology-based power converters which are forwarded converters, push-pull hybrid converters, full bridge dual switch DC-DC converters, half-bridge power converters, and flyback converters.

The forward converter is one type of isolated converter that utilize the transformer for reducing the supply voltage requirement and increasing the load voltage demand. The forward converters are more reliable, plus high flexible when associated with the flyback converter (Wang et al., 2019). The disadvantages of forward converters are suitable only for low-power applications, required a greater number of passive components, and have high difficulty in understanding. The flyback converter can be used for AC-DC and DC-DC power conversion. In this converter, galvanic isolation is used at the input port, and output ports. The features of a flyback converter are high energy storage by the transformer itself, less noise, less components count, space-saving, and good transient response (Goudarzian et al., 2022). The disadvantages of this converter are lower working efficiency, significant heat generation, plus required heat sink for mounting on switches. The push-pull power converter is used in hybrid solar/PEMFC power distribution networks for reducing the switching losses and gives a steady-state supply current (Musumeci and Di Mauro, 2017). In this converter circuit, the galvanic isolated transformer gives various step-up ratios, a high ability to control the various output voltages by using a single controller, and reduced power semiconductors count.

The push-pull DC-DC converter drawbacks are high complexity in the design of the transformer and high switching voltage. The half-bridge isolated type DC-DC converter is used in high-power-rated industrial applications (Wu et al., 2017). The merits of this converter circuit are the high utilization factor of the transformer, gives good operating performance, most suitable for moderate power applications, and less output current ripple. The disadvantages of this converter are high transient response, and cross conduct of switching's are possible. To limit the disadvantages of the half-bridge converter, a full-bridge isolated converter is applied in the article Wei et al. (2020) for reducing the output current ripples. The merits of this converter are high working efficiency, high input voltage, less voltage stress, and required a smaller number of passive elements to design. But, the implementation cost of this converter is very high. The switched-mode power converters work as a regulated power supply (Naik et al., 2016). The features of switched converters are high efficiency, more flexibility for industrial applications, and compactness in size. The main disadvantage of this converter is high-frequency noise.

In the article Elsayad et al. (2019), the voltage multiplier-based single switch DC-DC converter is used to obtain the high voltage conversion ratio of the fuel stack. This converter works with zero current switchings and reduced voltage stress on diodes. The reverse recovery current of the diode is optimized by using the voltage multiplier circuit. Also, the multiplier circuit works as a filter to suppress the distortions of converter output voltage. In the article Fuzato et al. (2016), the three-stage commutation-based converter is interfaced in the fuel cell battery charging network for eliminating the switching, plus conduction losses of the hybrid power generation system. Due to the two active switches of the converter, it works for high, and medium-power applications. However, the drawbacks of the above-isolated power converters are compensated by utilizing the conventional DC-DC converter as shown in Fig. 2.

Table 1
Summary of previously proposed hybrid maximum power point tracking controllers.

Authors	Year	Sensing Parameters	Hybrid MPPT	Control Variable	Type of Converter	Contribution
Khan and Mathew (2019)	2019	Fuel cell temperature& current	Fuzzy controller	Duty cycle	Bidirectional DC-DC converter	The fuzzy logic controller is used in this work for obtaining the optimum duty value of the bidirectional DC-DC converter. Here, the hybrid PV/wind/fuel cell system is studied at different water membrane conditions, and it is investigated with the combination of the P&O controller.
Badoud et al. (2021)	2021	Fuel cell current, & voltage	BG with FLC	Duty cycle	SEPIC Converter	Here, the authors proposed the Bond Graph-based fuzzy logic MPPT controller for enhancing the efficiency of PEM fuel cells at different atmospheric conditions. The merits of this controller are low oscillations across MPP, greater efficiency, less steady-state error in converter voltage, and high convergence speed. The hybrid controller is compared with the PSO, P&O, and FLC.
Basha and Rani (2022)	2022	Voltage & Current	Improved Beta with FLC	Duty cycle	Single Switch Boost Converter	In this work, the authors utilized the enhanced beta value-based fuzzy controller for extracting the maximum power from the fuel stack. In this hybrid controller, initially, the beta constraint is used to move the working point of the fuel stack near the actual MPP position. Later, the fuzzy controller is applied for optimizing the steady state error of the MPP.
Safarishaal and Sarvi (2023)	2023	Temperature, and Voltage	ICA with ANN	Duty cycle	Buck-Boost Converter	The Imperialist Competitive Algorithm trained Artificial Neural Network (ICA with ANN) is proposed for generating the quality power supply from the fuel stack at multiple temperature conditions. The hybrid algorithm is compared with the ANFIS controller in terms of MPP tracking speed, and maximum power extraction.
Hai et al. (2023)	2023	Temperature, and water membrane	MFSO with fuzzy	Duty cycle	Boost Converter	The Modified Fluid Search Optimization (MFSO) approach and Fuzzy Logic Controller (FLC) are used in this article for tracking the MPP at fast changes of temperature, and water membrane conditions. The features of this hybrid controller are high convergence speed, reduced oscillations, and high accuracy.
Reddy et al. (2023)	2023	Voltage, and Current	RBF with FLC	Duty cycle	Conventional Boost Converter	In this article, a Radial Basis Functional Network optimized fuzzy logic controller is introduced for the hybrid PV/fuel cell system to control the duty cycle of the DC-DC converter. The merits of this controller are high voltage gain, more efficiency, and less training time required for tracking the MPP.
Ali et al. (2023)	2023	Temperature, Water membrane, and Current	MMRF with FLC	Duty cycle	Buck-Boost Converter	Here, the Modified Manta-Ray Foraging Optimization-based ANFIS MPPT controller is proposed for enhancing the working efficiency of the fuel cell at different atmospheric conditions. The optimization controller selects the duty cycle value for the step-up of the fuel cell-generated voltage.

The rest of the article is organized as follows: in Section 2, the literature review of hybrid MPPT techniques is presented in terms of tracking speed, oscillations across MPP, and settling time of the MPP. In Section 3, the mathematical design, and performance analysis of proton exchange membrane fuel cell have been discussed. In Sections 4 and 5, the design of different hybrid MPPT techniques, and DC-DC converters have been presented. Finally, in Sections 6 and 7, the simulation results, and comprehensive analysis of hybrid MPPT techniques are explained.

2. Literature survey on MPPT techniques

The adaptive Incremental Conductance (IC) power point tracking controller is used in the article Azri et al. (2017) for the fuel stack-based grid-tied system in order to enhance the efficiency of the overall fuel cell system at various water membrane conditions. Here, the slope of the fuel stack curve is used for moving the operating point of the fuel cell near the actual MPP position. If the slope of the V-I curve is positive then the working point of the fuel cell is on the left side corner of the MPP. Or else, the operating point of the fuel cell is at the right corner of the MPP. The features of the IC controller are single sample is needed for selecting the decision, and required less settling time of MPP when compared to the conventional P&O power point tracking controller (Alaraj et al., 2017). But this method is having the disadvantage of high implementation cost. Also, this method requires high computational time and high-power loss. There are a few more hybrid MPPT controllers discussed in Table 1 for the fuel cell power generation system.

In the article Chen et al. (2017), the researchers focused on the adjustable step value IC controller for fast identification of the MPP position of the fuel stack. The main aim of this technique is the selection of variable step values for limiting the transient response of the entire system. The Hill Climb (HC) working behavior is nearly equal to the adaptive P&O technique. The main difference between these two techniques is DC-DC converter duty cycle control (Ghoshal et al., 2022). The advantages of HC are well suitable for particular complex -problem solutions, no need for any objective function, and very fast action. The HC gets suffers from the continuous variation of water membrane content, and less accuracy in MPP position. The Incremental Resistance (IR) controller is used in hybrid renewable power supply systems for enhancing the MPP tracking accuracy of fuel cells. Also, this controller is suitable for static, and dynamic temperature conditions. The IR has been applied in most of the practical real-world complex issues solutions because of its wide operating range (Rezk and Fathy, 2020). Here, the IR adjustable step value is analyzed with a constant step value in terms of convergence speed, power point tracking time, converter power losses, and implementation complexity. Based on the IR-fed fuel stack interfaced DC-DC converter output voltage waveforms, the adjustable step incremental resistance MPPT controller gives superior performance when compared to the IC (Rezk, 2016).

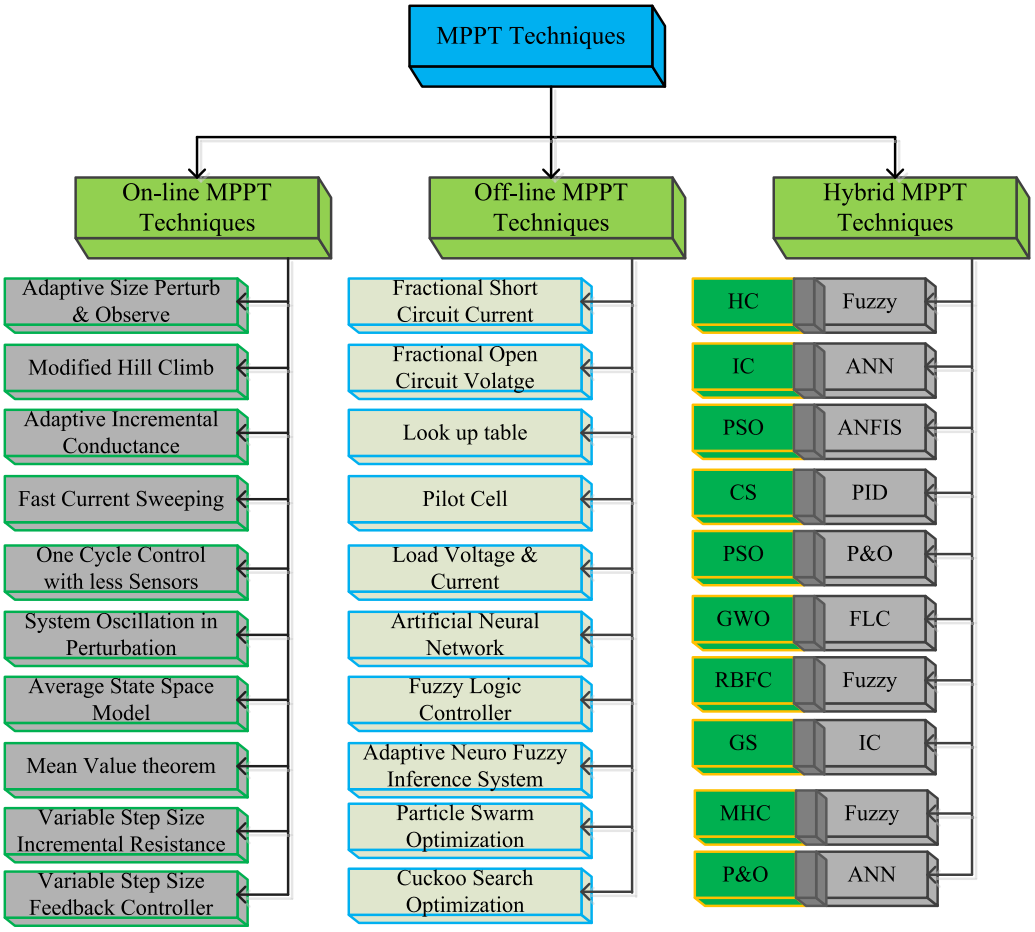

Fig. 3. Differentiation of hybrid, online, and offline MPPT controllers, (Kiran et al., 2022).

The slider MPPT controller is used in the PEM fuel stack system for solving the issue of MPP oscillations. The slider controller enhances the fuel stack-generated output voltage by utilizing the filter in the half-bridge interleaved boost converter (Souissi, 2021). The merits of the slider controller are maximum power extraction, parallel efficient current sharing in the DC-DC converter, and regulation of interior voltage for maintaining the constant fuel cell voltage. Also, the slider controller is useful for dc-link voltage regulation of the converter, voltage balancing at grid terminals, and local load power factor correction. However, the disadvantages of the slider controller are high design costs and more difficulty in understanding the operation. In article El Otmani et al. (2020), the authors utilized the extended sliding controller for a battery-operated fuel cell system to maintain the constant supply voltage of the grid. This improved slider MPPT technique is more suitable for hybrid EV-fed induction motor drive applications. The merits of an improved slider controller are less dependent on fuel cell operation, the moderate settling time of MPP at constant temperature values, and fast system response (Kanouni and Mekhilef, 2022b). The drawback of this extended slider controller is high oscillations across MPP at dynamic operating temperature conditions of the fuel stack (Silaa et al., 2020).

In the article Nureddin et al. (2020), the authors used the neural network-based MPPT controller for the hybrid fuel cell, and solar power generation system for charging the battery. In this neural network controller, the selected input variables are fuel cell voltage, solar Photovoltaic (PV) voltage, fuel cell current, and solar PV current. In order to find out the suitable duty cycle for the DC-DC converter, there are six thousand data samples are collected for training the network. The features of these neural network controllers are easy to understand, less complexity in design, and have high flexibility (Srinivasan et al., 2021). The drawbacks of this MPPT controller are high steady-state oscillations of converter output voltage. So, most of the research scholars working on hybrid power point tracking controllers for fast-tracking of MPP, less settling time of converter output voltage, and high efficiency (Rafikiran et al., 2023). The classification of online, offline, and hybrid MPPT controllers are shown in Fig. 3.

3. Mathematical design, and analysis of PEMFC

As of now, there are different types of fuel cell working behavior analyzed in the literature survey. From the literature review, it is identified that the proton exchange or polymer electrolyte-based fuel stack gives more advantages when compared to the other conventional fuel cell technologies (Bargal Mohamed et al., 2020). The advantages of PEMFC are a very less starting time, good flexibility, excellent thermal stability, and high safety. Pure methanol, formic acid, plus hydrogen are the inputs to the selected fuel cell stack. The proposed PEM fuel stack applications are stationary, transportation, plus portable (Awin and Dukhan, 2019). The architecture of PEMFC is given in Fig. 4a, and its equivalent circuit is given in Fig. 4b. From Fig. 4a, the hydrogen (H_2) is transferred to proton ions ($2H^+$) with the help of the catalyst surface, and it gives the electrons to the external circuit through an anode chamber.

The fuel cell stack chemical actions at the anode and cathode chambers are derived as (Kiran. et al., 2022),

$$H_2 \Rightarrow 2H^+ + 2e^- \quad (1)$$

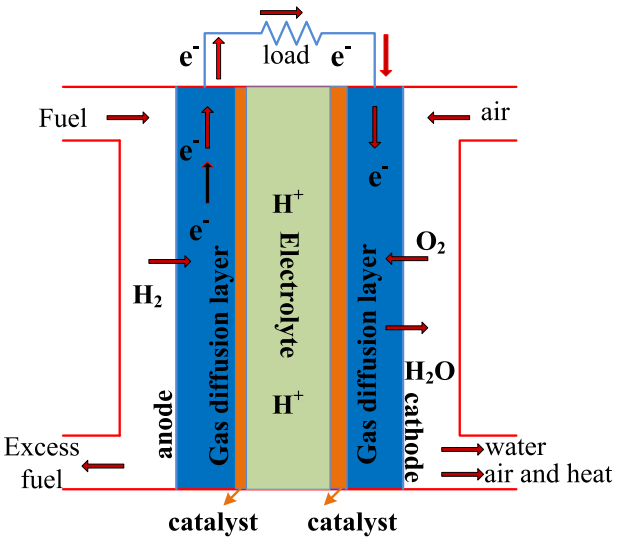

Fig. 4a. Chemical reactions of the PEM fuel cell.

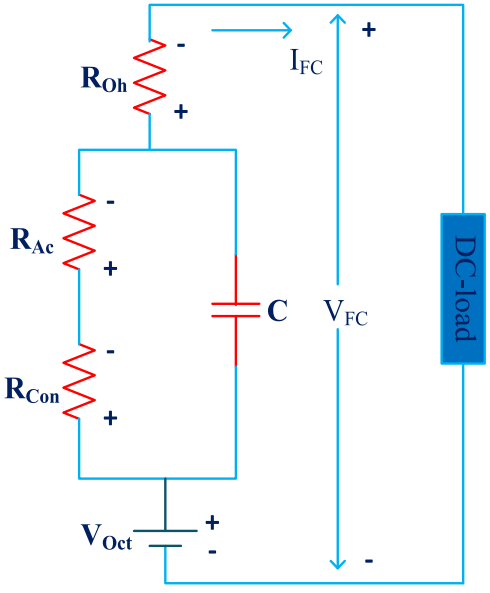

Fig. 4b. Equivalent circuit of PEM fuel cell.

$$2H^+ + 2e^- + \frac{1}{2}O_2 \Rightarrow H_2O \tag{2}$$

$$H_2 + \frac{1}{2}O_2 \Rightarrow H_2O + E \tag{3}$$

$$V_T = N{*}V_{FC} \tag{4}$$

$$V_{FC} = E_{0ct} - V_{Oh} - V_{Ac} - V_{Con} \tag{5}$$

$$E_{Oct} = 1.29 - 0.8e^{-3}\left(T_{FCope} - 298.12\right) + 4.3e^{-5}\log(P_{H_2}\sqrt{P_{O_2}})T_{FCope} \tag{6}$$

There are '*N*' number of fuel cells used to design the fuel stack. From Eq. (4), the total fuel stack voltage (V_T) is equal to the total number of fuel cells by the multiplication of each fuel cell voltage (V_{FC}). From Eq. (5), the 'E_{Oct}'' is defined as the thermodynamic potential at the open circuit condition of the fuel stack. The terms V_{oh}, V_{Ac}, and V_{Con} are the fuel cell ohmic, active, and concentrated polarization losses (Kurnia et al., 2021). From Eq. (6), the term T_{FCope} is defined as each cell working temperature. The partial parameters of hydrogen and oxygen are defined as (P_{H_2}), and (P_{O_2}). From Eq. (7), the parameters RH_{Ano}, 'I_{cell}', $P_{Ano,}$ and '*A*' are defended as humidity vapor of anode at reverse working conditions, fuel cell generated output current, inlet anode chamber, and electrode cross-sectional area. The terms RH_{Cat}, and P_{Cat} are defended as humidity vapor at the cathode, and inlet chamber of the cathode. The empirical coefficients of the PEM fuel cell are K_1, K_2, K_3, and K_4. The supplied concentration-based oxygen (C_{O_2}) is derived as (Ahmad et al., 2022),

Table 2
Design parameters of the proposed fuel cell system at various temperature conditions.

Constraints	*Values*
Selected power of the fuel stack	6.0 kW
Oxygen pressure in partial condition	1.00 bar
Hydrogen pressure at the partial condition	1.500 bar
Overall utilized fuel cells (N)	65.0
Voltage of fuel cell stack at open circuit state	65 V
Voltage of fuel cell at peak power point (V_{MPP})	45.0 V
Current of the fuel cell at peak power point (I_{MPP})	133.33 A
Basic air passing rate (I_{pm})	506.40
Constant value of gasses (R)	84.092 [J mol^{-1} K^{-1}]
Constant of faraday (F)	95,432.218 [C mol^{-1}]
Composition levels of fuel cell	99.95%
The consumption level of oxygen	59.3%

$$P_{H_2} = \frac{1}{2}RH_{Ano}{*}P^{sat}_{H_2O}\left(\frac{1}{\frac{RH_{Ano}P^{sat}_{H_2O}}{P_{Ano}}\exp\left(\frac{1.6(I_{cell}/A)}{T_{FCope}}\right)}\right) \tag{7}$$

$$P_{O_2} = \frac{1}{2}RH_{Cat}{*}P^{sat}_{H_2O}\left(\frac{1}{\frac{RH_{Cat}P^{sat}_{H_2O}}{P_{Cat}}\exp\left(\frac{4.10{*}(I_{cell}/A)}{1.33{*}T_{FCope}}\right)}\right) \tag{8}$$

$$V_{Ac} = K_1 + K_2T_{FCop} + (K_3 + K_4)T_{FCope}\log(C_{O_2} + I_{cell}) \tag{9}$$

$$V_{Con} = -\frac{RT_{FCope}}{N * F}\log(1 - \frac{X}{X_{max}}) \tag{10}$$

$$V_{Oh} = I_{cell}{*}(R_{ef} + R_{pf}) \tag{11}$$

$$C_{O_2} = \frac{P_{O_2}}{5.08e^6\exp(-498/T_{FCope})} \tag{12}$$

$$j = \frac{I_{cell}}{A} \tag{13}$$

$$R_{ef} = \frac{\gamma_{ef} * Q}{A} \tag{14}$$

From Eq. (10), the terms '*R*', '*F*', and '*X*' are defended as hydrogen gas constraint, faradays constant, and fuel cell cross over. The terms R_{ef}, and R_{pf} are the effective resistances of electrolyte and water membrane content. From Eq. (12), and (13), the terms P_{O_2}, j, Q, and r_{ef} are defended as the partial pressure of oxygen, current density, rate of charge, and specific resistivity (Deng and Li, 2022). The proposed proton exchange membrane fuel cell system design values are given in Table 2. Based on Table 2 parameters, the fuel cell generated V-I, and P-I characteristics are shown in Fig. 5(a), and (b). From Fig. 5(a), it is identified that the peak current and voltage of the fuel stack are 133.3 A and 45 V which indicates that the current passing through the proposed system is more. So, the fuel stack supply voltage is improved by using the DC-DC converter.

4. Performance analysis of various MPPT controllers

The fuel cell gives nonlinear voltage versus current characteristics. So, the extraction of maximum power from the fuel stack is quite difficult (Grumm et al., 2020). To transfer the maximum power from supply to load, a maximum power point tracking

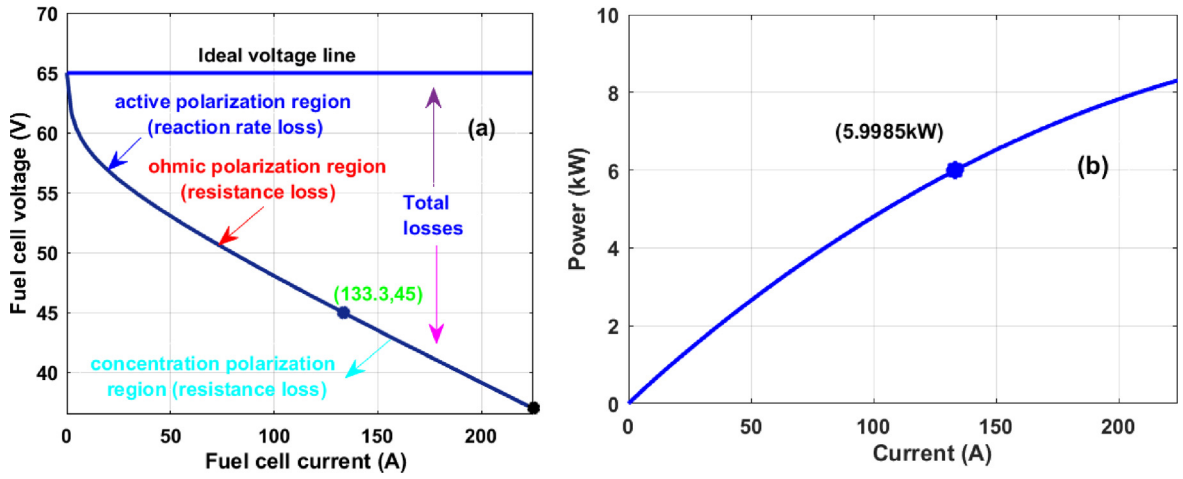

Fig. 5. Fuel stack nonlinear, (a). V-I characteristics, and (b). P-I Characteristics.

controller is used for the enhancement of fuel stack performance. Here, a grey wolf algorithm optimized fuzzy system is proposed for finding the functioning point of the fuel stack, and it is compared with other conventional MPPT methods such as Adaptive Adjustable Step-P&O (AAS-P&O), Variable Step Value-Radial Basis Function Controller (VSV-RBFC), Improved HC dependent Fuzzy System (IHC with FS), plus P&O correlated Particle Swarm Optimization (P&O with PSO).

4.1. Adaptive adjustable step-based P&O controller

From the previously published articles, the basic P&O technique is a commonly utilized power point tracking controller for the continuous tracking of the MPP position of the fuel stack (Yuan et al., 2020). The merits of the P&O method are easy to design, simple in understanding, and has high convergence speed. The drawbacks of the P&O controller are high oscillations at MPP and less accuracy in MPP tracking. To compensate for the drawbacks of the P&O controller, in the article Gugulothu et al. (2022), the authors applied the adaptive adjustable step value based perturb and observe controller for the fuel stack fed boost converter system. In this controller, at starting, a high step value is utilized for the fast convergence speed. Slowly, the convergence speed is reduced by reducing the step value. As a result, the distortions in converter voltage are optimized. However, the drawbacks of this MPPT controller are high power losses at the time of perturbation, and less applicable for hybrid fuel stack, and battery-charged EV systems. The selected input signals for the P&O controller are fuel cell current, and voltage (Kanouni and Mekhilef, 2022a). The fuel stack voltage is enhanced by adjusting the duty cycle of the DC-DC converter. The duty is controlled with the help of the equivalent resistance of the fuel stack.

The DC-DC converter duty cycle updating has been done by using Eq. (15), and (16). From Eq. (15), the duty (D) of the power converter is updated when the functioning point of the fuel stack is at the left-hand side of the actual MPP position. So, the converter duty cycle is increased for improving the voltage profile of the fuel cell system. If the functioning point is on the right side of the V-I curve then the converter duty is decreased by using Eq. (16). Finally, the utilized constant (ς) is used for the adjustment of step value on nonlinear V-I characteristics of the fuel cell. The parameters D (n-1), and D (n) are the previous, and present duty cycle values of the DC-DC converter. Similarly, the terms p (n-1), p (n), v (n-1), and v (n) are the past, and present power, and voltages of the fuel cell.

$$D(n) = D(n-1) + \varsigma * \left(\frac{p(n) - p(n-1)}{v(n) - v(n-1)}\right) \tag{15}$$

$$D(n) = D(n-1) - \varsigma * \left(\frac{p(n) - p(n-1)}{v(n) - v(n-1)}\right) \tag{16}$$

$$\text{step\_vary} = \varsigma * \left(\frac{p(n) - p(n-1)}{v(n) - v(n-1)}\right) \tag{17}$$

4.2. Variable step value-radial basis functional MPPT controller

From the previously published articles, neural networks are the most utilized soft computing methods for nonlinearity behavior-related problem-solving applications. The neural network data is trained by utilizing the two popular techniques which are illustrated as unsupervised, and supervised methods. The unsupervised methodology is applied to the system to train the input variables data, and the radial function is utilized for the tuning of the fuel cell parameters (Girirajan et al., 2022; Gopal and Meenendranath Reddy, 2023). The working structure of the radial basis functional network is shown in Fig. 6. From Fig. 6, it has been identified that the neural network controller consists of three layers which are illustrated as the input layer, middle, plus output side layer. The input layer consists of different nodes which receive the data from the fuel stack. The input side nodes of the neural network controller are indicated as signal transmitters (Yahia et al., 2022). The hidden layer consists of a radial basis function which works as a nonlinear problem-solving function of the fuel cell system. The main objective of a radial function is an approximation of multivariate functions into a single unvaried function. Here, the radial network works based on the cover theorem, and it casts the overall data into a multidimensional space by utilizing the middle layer.

So, the middle layer neurons are quite higher than the input side neurons. The radial basis function value is measured in terms of distance which is obtained from the origin. The radial function effect must and should contain the real values activation functions. The output of the neural network consists of a single node that gives the duty signal to the fuel stack-fed DC-DC power converter system for enhancing the power extraction capability of the fuel cell. The supervised concept is applied to the input layer nodes for giving the random weights, and those are upgraded step by step by utilizing the activation function. The weight adjustment of all nodes is obtained as (Su et al., 2023),

$$I_P^1(i) = f_P^1(net_P^1(i)) = net_I^1(i) \quad i = 1, 2, ..n \tag{18}$$

$$net_R^2(i) = -(k - G_R)^T \sum_m (k - G_R);\ i = 1.2.3.., n \tag{19}$$

$$I_R^2(i) = f_R^2(net_R^2(i)) = net_R^2(i);\ i = 1.2.3.., n \tag{20}$$

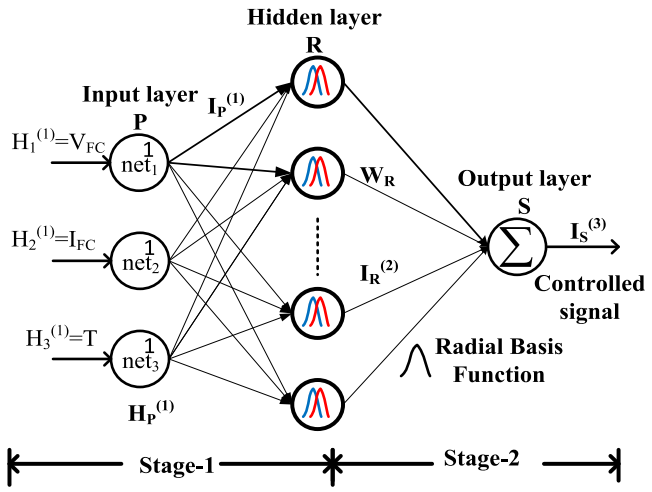

Fig. 6. Architecture of radial function MPPT technique for fuel cell (Rajesh, 2023).

Where the terms I_P^1, 'i', and $net_p^1(i)$ are represented as the overall input of the first layer, the total number of iterations, and net value of input of each node. Similarly, in the middle layer, the net input and its related outputs are obtained by utilizing Eq. (19) and (20) (Su et al., 2023). From Eq. (19), the terms net_R^2, K and G_R are defended as the net output of the middle layer, standard value, and standard deviation value. The output layer net output, and input are determined as net_s^3, and I_s^3. In addition, every node in the hidden layer works as a Gaussian membership function. From Fig. 6, it has been identified that the final layer consists of a single node and its related output signal is obtained by utilizing the various nonlinear activation functions. The net value of the output layer is derived as (Pasternak and Bresser, 2022),

$$net_S^3 = \sum_R W_R * y_R^2(i);\ i = 1.2.3..,\ n \tag{21}$$

$$I_S^3(i) = f_S^3(net_S^3(i)) = net_S^3(i);\ i = 1.2.3\ldots,\ n \tag{22}$$

$$H = \begin{bmatrix} H_1 & H_2 & H_3 & \ldots H_n \end{bmatrix} \tag{23}$$

$$I = \begin{bmatrix} I_1 & I_2 & I_3 & \ldots I_n \end{bmatrix} \tag{24}$$

Where '*n*' is the total number of samples that are selected as 629. The error signal of the proposed power point finding controller is derived in terms of reference, and maximum voltage of the fuel stack. From Eq. (23), and (24), the terms '*H*', and '*I*' denotes the fuel cell voltage, and current vectors (Jianfeng et al., 2023).

$$error = \sum_{k=1}^{n} \frac{1}{2} (V_{ref} - V_{MPP}) \tag{25}$$

4.3. Improved HC-dependent fuzzy MPPT technique

Hill Climb is one of the most popular conventional controllers for identifying the MPP position of the fuel stack at different temperature conditions (Hussaian Basha and Rani, 2020). The HC MPPT controllers are local search controllers. The drawbacks of the HC technique are less suitable for dynamic operating temperature conditions of the fuel cell, high distortions in converter output voltage, and less tracing speed. The working structure of the HC-based fuzzy power point finding controller is shown in Fig. 7. To limit the disadvantages of the HC controller, the improved hill climb-dependent fuzzy logic controller is used in the article (Bigdeli, 2015) for continuous tracking of fuel cell MPP at various supply temperature values. Here, the HC working concept is transferred into 16 fuzzy rules, and these are divided into 4-subsets as illustrated in Fig. 7. From Fig. 7, the fuzzy rules are identified as Positive Large (PL), Positive Moderate (PM), Negative Moderate (NM), plus Negative Large (NL). The features of this hybrid power point identifying controller are high tracing speed, moderate power loss at V-I slope step variation, good dynamic response, and less convergence time. However, the disadvantage of this controller is the high fluctuated converter output voltage.

4.4. P&O correlated PSO power point finding controller

As from the above conventional power point tracking techniques, the P&O is a frequently utilized controller for finding the required working operating point of the fuel cell. In article Rajesh et al. (2021), the authors focused on the combination of P&O with PSO controller for limiting the disadvantages of the basic conventional P&O technique. Here, at the initial state, the P&O controller is utilized for moving the operating point of the fuel cell to the actual MPP position. So that the hybrid controller tracing speed is improved. After completion of the P&O operation, the PSO controller works to limit the distortions of the operating point of the fuel stack. The working flowchart of the hybrid P&O with PSO controller is given in Fig. 8 (Hussaian Basha et al., 2022).

The features of this hybrid MPPT controller are high operating efficiency, more accuracy, less time for the initialization of the length of the article, less power loss, and good performance. At starting, in this PSO technique, all the swarm particles are selected as agents which search the entire search space for obtaining the required duty cycle of the DC-DC converter. In this searching time duration, each particle exchanges its searching information with each other to track the MPP. Here, the particles move randomly in different directions at the first iteration. After that the complete multiple iterations, the particle runs in one direction toward the required object.

$$V^{x+1} = WV_k^x + c_1a_1(P_b - y_k^x) + c_2a_2(G_b - y_k^x) \tag{26}$$

$$y^{x+1} = y_k^x + V_k^x \tag{27}$$

The particle velocity and length are adjusted by utilizing Eq. (26), and Eq. (27). From Eq. (26), it is identified that the parameters 'V', 'W', and 'y' are named as swarm velocity, weight, and length. Also, the terms 'x', and 'k' are identified as particle iteration and position. Each particle's best position is determined as 'P_b', and the overall particle's exact position is identified as 'G_b'. The major drawback of this hybrid controller is low convergence speed and less accuracy in more search space regions. From Fig. 8, the terms $V_{Max}(x)$, $I_{Max}(x)$, and $P_{Max}(x)$ are indicated as maximum fuel cell voltage, current, and power at P&O working conditions. Similarly, the term P(y) is indicated as fuel cell power which is obtained by using the PSO controller.

4.5. Variable step GWA-fuzzy logic controller

The drawbacks of the above power point tracking techniques are overcome by using the variable step GWA-based fuzzy logic controller. Here, the disadvantages of GWA, and fuzzy are neglected for the implementation of the hybrid MPPT controller. The grey wolf controller is the one of most popular meta-heuristic controllers which works based on the grey wolf imitating behavior in nature (Basha et al., 2023). The wolf is cooperatively starting the hunting. The major difference between the grey wolf optimization technique and other optimization techniques are structure modeling and rate of convergence. The GWA is used in many applications which are complex nonlinear problem-solving, and automotive industry applications. The mathematical equitation of GWA is obtained from the social hierarchy wolfs.

$$\left.\begin{array}{c} if\ Delta\ P\ is\ >0 \\ if\ Delta\ I\ is>0 \\ D(y)=D(y-1)+Delta\ D \\ else \\ D(y)=D(y-1)-Delta\ D \\ end \end{array}\right\} \rightarrow \left\{\begin{array}{l} if\ DeltaP\ is\ PL\ and\ DeltaI\ is\ PL\ then\ Delta\ D\ is\ PL \\ if\ DeltaP\ is\ PL\ and\ DeltaI\ \ is\ PM\ then\ Delta\ D\ is\ PL \\ if\ DeltaP\ is\ PL\ and\ DeltaI\ \ is\ NL\ then\ Delta\ D\ is\ NL \\ if\ DeltaP\ is\ PL\ and\ DeltaI\ \ is\ NM\ then\ Delta\ D\ is\ NL \\ if\ DeltaP\ is\ PM\ and\ DeltaI\ \ is\ PL\ then\ Delta\ D\ is\ PM \\ if\ DeltaP\ is\ PM\ and\ DeltaI\ \ is\ PM\ then\ Delta\ D\ is\ PM \\ if\ DeltaP\ is\ PM\ and\ DeltaI\ \ is\ NL\ then\ Delta\ D\ is\ NM \\ if\ DeltaP\ is\ PM\ and\ DeltaI\ is\ NM\ then\ Delta\ D\ is\ NM \end{array}\right.$$

$$\left.\begin{array}{c} elseif\ Delta\ P\ is<0 \\ if\ Delta\ I\ is>0 \\ D(y)=D(y-1)-DeltaD \\ else \\ D(y)=D(y-1)+Delta\ D \\ end \end{array}\right\} \rightarrow \left\{\begin{array}{l} if\ DeltaP\ is\ NL\ and\ DeltaI\ is\ PL\ then\ Delta\ D\ is\ NL \\ if\ DeltaP\ is\ NL\ and\ DeltaI\ is\ PM\ then\ Delta\ D\ is\ NL \\ if\ DeltaP\ is\ NL\ and\ DeltaI\ is\ NL\ then\ Delta\ D\ is\ PL \\ if\ DeltaP\ is\ NL\ and\ DeltaI\ is\ NM\ then\ Delta\ D\ is\ PL \\ if\ DeltaP\ is\ PM\ and\ DeltaI\ is\ PL\ then\ Delta\ D\ is\ NM \\ if\ DeltaP\ is\ PM\ and\ DeltaI\ is\ PM\ then\ Delta\ D\ is\ NM \\ if\ DeltaP\ is\ PM\ and\ DeltaI\ is\ NL\ then\ Delta\ D\ is\ PM \\ if\ DeltaP\ is\ PM\ and\ DeltaI\ is\ PM\ then\ Delta\ D\ is\ PM \end{array}\right.$$

Fig. 7. An adaptive hill climb-dependent fuzzy logic controller.

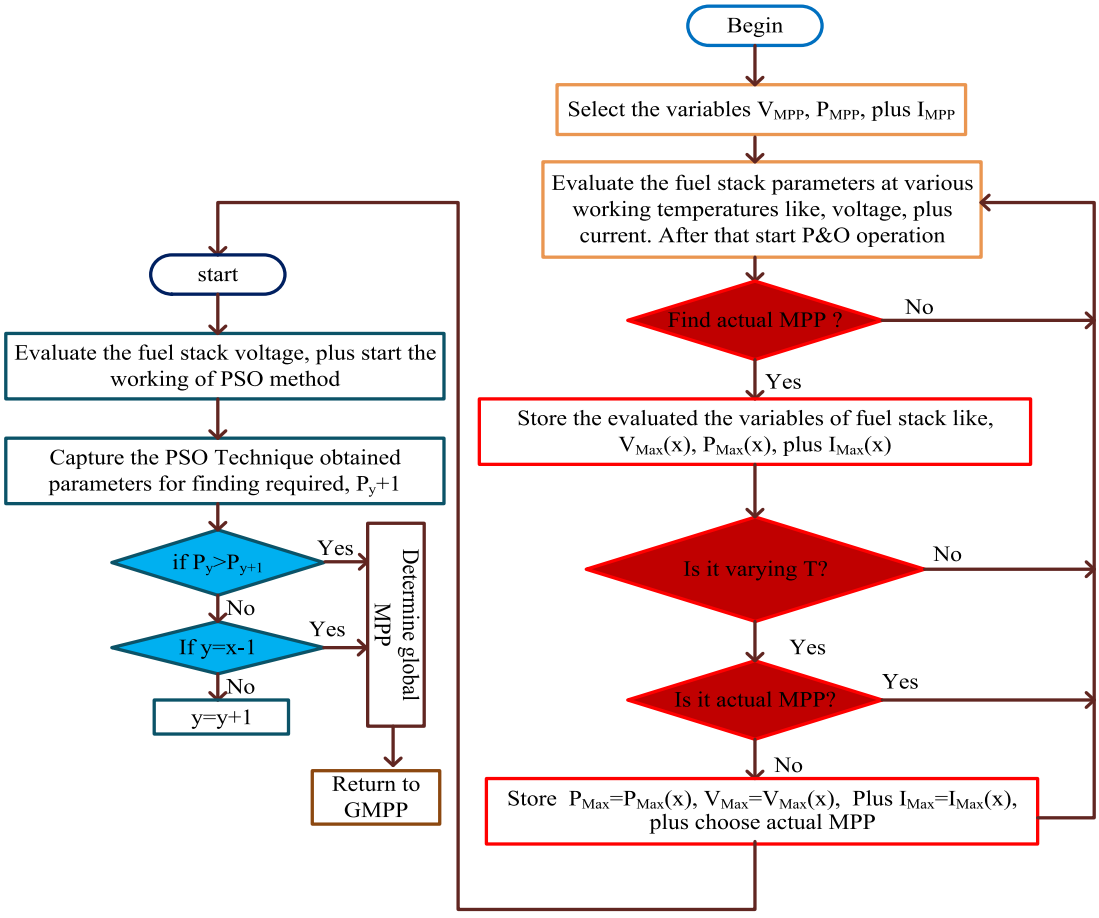

Fig. 8. Hybrid conventional-based PSO power point identifying the controller.

Here, there are different fitness functions selected in the GWA which are the first fitness function is named α, and the second, and third are represented as β, plus δ. Also, the remaining wolf's optimum solution is selected as ω. In this hybrid MPPT controller, initially, a GWA is utilized for finding the local working point of the fuel stack at fast changes in operating temperature conditions. At this time, the working point of the fuel stack closely moves to the required MPP place to limit the convergence time of the controller (Rana et al., 2019). The features of GWA are good accuracy, fast running speed, and less dependence on the working behavior of the fuel stack. The only demerit is high fluctuations of MPP which is overcome by combining the fuzzy controller with the GWA. The flowchart of the hybrid power point tracking controller is given in Fig. 9, and its corresponding Pseudo code is given in Fig. 10. From Fig. 10, it has been seen that the wolf is initialized randomly with various values. After the completion of multiple iterations, it gives an MPP position at continuous changes in operating temperature values. The condition of fuel stack error

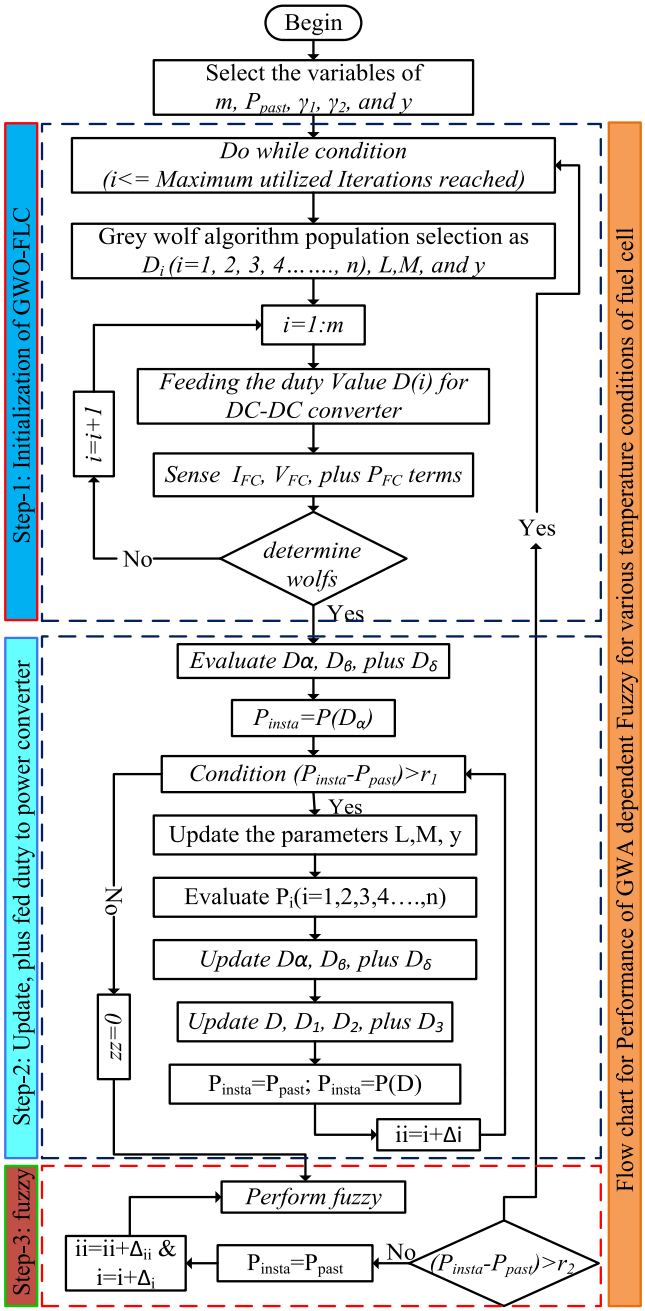

Fig. 9. Proposed grey wolf technique-based fuzzy MPPT controller.

voltage and currents is given to the fuzzy logic controller which is derived as,

$$\left|P_{insta} - P_{past}\right| \leq \gamma_1 \tag{28}$$

$$\left|P_{insta} - P_{past}\right| \geq \gamma_2 \tag{29}$$

Where, the P_{insta}, P_{past} are defined as the instantaneous, and past maximum powers of the fuel cell. The limiting factor r_1 is utilized to supply the output of the GWO controller to the fuzzy block. The utilizing limiting factor value in the proposed MPPT method is 0.04. In the same manner, the fuzzy output power error signal is fed to the grey wolf controller by utilizing Eq. (28). Where r_2 is indicated as the limiting factor which is selected as 0.06. Based on the limiting factor, the fuzzy signal is feedback to the grey wolf controller for maintaining the constant MPP position. From Fig. 11, the fuzzy is collecting error variables, which are converted from real variables to linguistic variables by applying the fuzzification system. In the fuzzification block, there are seven membership functions are utilized as shown in Table 3. The min–max inference block is utilized for forming the knowledge base rules. The max-term is used for the addition of all generated output rules, and the min-term is applied for fuzzy concept implementation.

5. Design of conventional DC-DC converter

As of from the literature review, the isolated power converters are having the drawbacks of high implementation cost, more size, heavy weight, more power losses, and more complexity in understanding. Also, these converters required additional power electronics circuits (Ali et al., 2014). As a result, the handling of ripple currents is very difficult in the power generation system. So, in this work, the conventional power DC-DC converter is

Table 3
Fuzzy logic rules for power point tracking controller.

	Change in fuel cell power (dP/dt)							
	e/Δe	NL	NM	NS	ZE	PS	PM	PL
	NL	NL	NL	NM	ZE	PM	PL	PL
	NM	NL	NM	NM	ZE	PM	PM	PL
Change in PV voltage (dV/dt)	NS	NL	NM	NS	ZE	PS	PM	PL
	ZE	ZE	ZE	ZE	ZE	ZE	ZE	ZE
	PS	PS	PS	PS	ZE	NS	NM	NL
	PM	PM	PM	PS	ZE	NS	NM	NL
	PL	PL	PL	PM	ZE	NM	NL	NL

Initial P_{past}=0,
Do while condition; i<= required iterations are very high
Initialize the Grey Wolf population D_m (i=1,2., n) here duty D_i is in the range of 0.19 to 0.98
Initialize the coefficient vectors L, y, and M for tracking MPP
Find out the every grey wolf fitness value P_i(i=1,2,..n)
D_α: is indicated as the initial best grey wolf.
D_β: is indicated as the second-best grey wolf.
D_δ: is indicated as the third-best grey wolf.
P_{insta} is equal to P (D_α)
  Do while condition, P_{insta}-P_{past} < γ_1
  Update the currently available grey wolf positions
  Update the coefficient vectors L, and M
  Find out each grey wolf's accurate fitness parameter P_i(i=1,2,..n)
  Adjust the values of the grey wolf D_α, D_β, plus D_δ
  Update the parameters D_1, D_2, plus D_3
  P_{insta}=P_{past}; P_{insta}=P(D_α)
  i=i+Δi
  End Do
  Ii=0
  Do while the condition of P_{insta}-P_{past} < γ_2
  Apply the fuzzy rules for identifying the required D, and P
  Ii=ii+Δ_{ii}
  End do
End do

Fig. 10. Pseudo code of hybrid power point tracking controller for fuel cell power generation system.

used for the study of various hybrid MPPT controllers at different operating temperature values of the fuel stack. The working of the conventional converter at forward and reverse bias conditions is shown in Fig. 12(a), Fig. 12(b). The features of this utilized converter are easy to design, high reliability, more flexibility, and less implementation cost. The conventional power converter works in two stages of operations which are forward bias, plus reverse bias. In the forward bias condition, the switch (Q) starts working, and the diode (D) stops working. The working time of the switch is represented as dT_S, and OFF time is represented as (1-d) *T_S. Here, the terms d, and T_S are represented as the duty cycle of the converter, and the conduction time of the switch. The volt-sec technique is applied across the inductor L_{fc} to find out the duty of the DC-DC converter which is given in Eqs. (30) and (31) (Kolli et al., 2015).

$$V_{fc} * dT_S + (V_{fc} - V_0) * (1 - d)\, T_S = 0 \tag{30}$$

$$-i_0 dT_S + (I_{fc} - I_0) * (1 - d)\, T_S = 0 \tag{31}$$

$$V_0 = \frac{V_{fc}}{(1-d)} \&,\ i_0 = i_{fc}\,(1-d) \tag{32}$$

6. Discussion of simulation results

Here, the conventional converter is interfaced for the implementation of the proposed fuel cell system. The selected input side capacitor C_{fc} is 42 μF which is acting as a supply voltage stabilizer at various working temperature conditions of the fuel cell. Also, this capacitor is helpful for load voltage ripple suppression. Similarly, the selected input inductor L_{fc} value is 20 mH. The input inductor suppresses the ripples in the fuel cell supply voltage. The MOSFET switch is used in the power converter for enhancing the input voltage of the fuel cell from one level to another level. Also, the converter reduces the fuel cell supply current. As a result, the entire system's heating losses are reduced. The selected values of load side resistor (R_0), capacitor (C_0), plus inductor (L_0) are 45 Ω, 40 μF, plus 40 mH respectively. Here, the proton exchange membrane fuel cell-based standalone system is studied at static, and dynamic operating temperature conditions of the fuel stack system.

6.1. Analysis of PEMFC-fed hybrid MPPT controllers at 340 K

The selected static temperature of the fuel cell for studying the different power point tracking controllers is 340 K as shown in Fig. 13. From Fig. 13, it has been seen that the static temperature conducting time duration of the fuel stack is 0.3 s Similarly, at 340 K temperature, the output power, current, plus voltages of the fuel stack system by applying adaptive step-based P&O, variable step-RBFC, and P&O-PSO-based MPPT techniques are 4929.9 W, 116.463 A, 42.33 V, 5118.99 W, 117.732 A, 43.48 V, 5353.22 W, 120.698 A, plus 44.36 V respectively. The working efficiency of fuel cells by applying the AAS-P&O, and VSGWA-based fuzzy techniques are 96.62%, and 98.44% respectively. The converter output power steady-state settling times by applying the radial basis controller, hybrid P&O-PSO, and variable step GWA-based fuzzy logic controller are 0.11 s, 0.14 s, and 0.143 s respectively.

The IHC with fuzzy, and RBF-based MPPT controllers are working based on the type of fuel cell selection. In addition, the RBF controller design, and implementation required high expert knowledge person to enhance its working performance. From Fig. 14(a), and (b), it is observed that the P&O, and RBFC MPPT controllers-based fuel cell output current, and voltage distortions are very high. As a result, the entire fuel stack system heating losses are increased. The advantages of these methods are less design complexity and easy understanding. From Fig. 14(c), at 340 K temperature, the obtained converter duty values by applying the VSV-RBFC, ASHC-fuzzy, and VSGWA-fuzzy based MPPT controllers are 0.66, 0.65, and 0.64 respectively. Here, the converter step-down the fuel cell current in order to reduce the overall system power losses. From Fig. 14(d), and (e), at 340 K working temperature of the fuel stack, the converter voltage, and current by applying the ASHC-fuzzy, VSGWA-fuzzy, and AAS-P&O are 562.8 V, 9.236 A, 563.93 V, 9.344 A, 556.71 V, and 8.556 A respectively. Also, from Fig. 14(e), it has been noted that the grey wolf optimized fuzzy logic controller gives a high voltage conversion ratio and less converter voltage rising time. Also, the performance efficiency of the GWA correlated fuzzy MPPT technique is 98.44% which is higher than the other power point tracking controllers as shown in Fig. 14(f). At 340 K, the extracted converter output power by applying the ASHC-fuzzy controller is 5198.411 W which is higher than the AAS-based VP&O and VSV-based RBFC controllers.

6.2. Analysis of PEMFC-fed hybrid MPPT controllers at 340 K, 320 K, and 300 K

Here, the PEM fuel cell-fed power converter is studied at dynamic operating temperature conditions by applying different MPPT controllers. From Fig. 15, it can be seen that the temperature of the fuel stack is 340 K up to the time duration of 0.3 s After

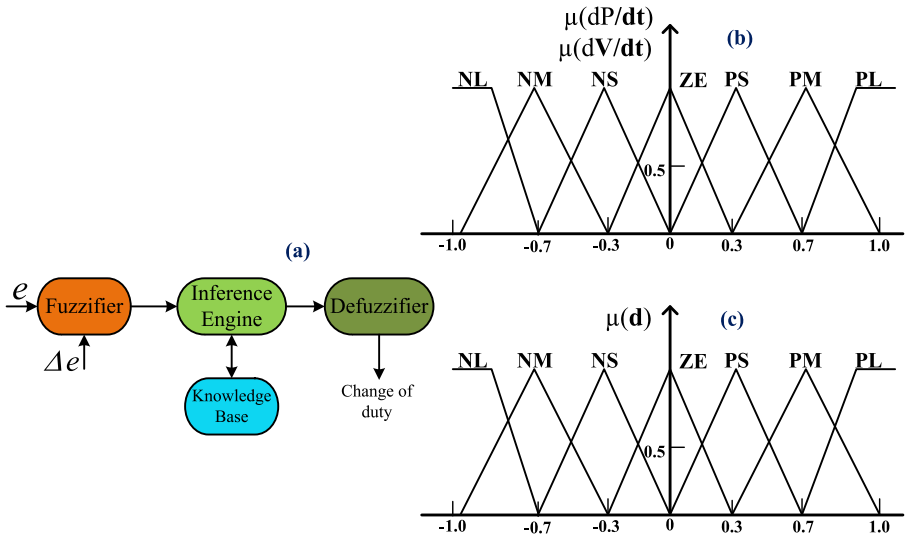

Fig. 11. (a). General operation of FLC, (b). Input variables membership functions, and (c). Output variable membership functions.

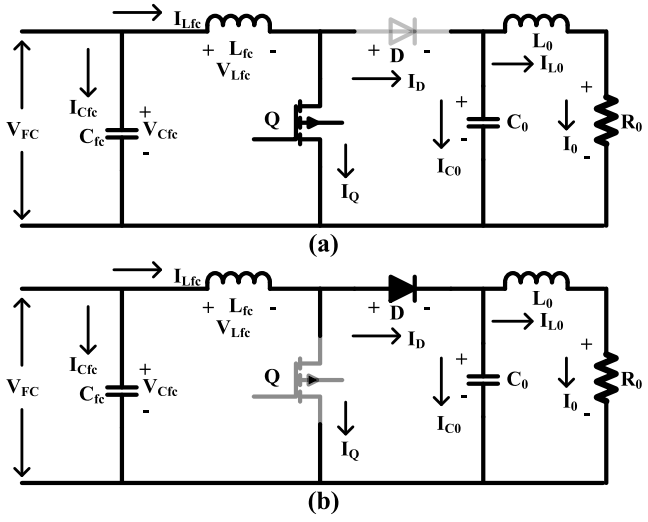

Fig. 12. Conventional converter under, (a). forward bias, (b). Reverse bias conditions.

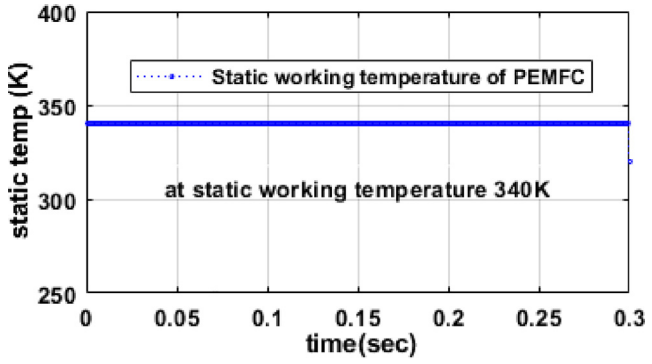

Fig. 13. Static operating temperature of proton exchange membrane fuel stack.

that, it is step-down to 320k up to the time duration of 0.6 s Finally, at 0.6 s, the temperature gets step-down to 300 K. At 340 K, the fuel cell generated output current, and voltage waveforms by utilizing the various power point tracking controller are shown in Fig. 16. At 340 K, from Fig. 16(a), it is observed that the fuel cell output current consists of different values by utilizing the various hybrid MPPT methods.

At 320 K, the extracted fuel stack voltage, power, and currents by applying the AAS-P&O, VSV-RBFC, and ASHC-fuzzy MPPT techniques are 39.88 V, 4430.12 W, 111.086 A, 40.92 V, 4599.31 W, 112.397 A, 42.31 V, 4777.99 W, and 112.928 A respectively. Similarly, the VP&O-PSO controller improves the fuel cell voltage from 42.59 V to 534 V by using a single switch power converter at 320 K as shown in Fig. 16(b). The VSGWA-optimized fuzzy controller extracts the maximum fuel stack power which is nearly equal to 4806.2 W, and it gives maximum efficiency at 320 K when compared to the VP&O power point tracking controller. The obtained duty values of the converter at 320 K by applying AAS-based P&O, VSV-based RBFC, ASHC-FLC, VP&O-PSO, and VSGWA-FLC MPPT techniques are 0.66, 0.668, 0.671, 0.674, and 0.675 as shown in Fig. 16(c). The converter output power, current, and voltage parameters are obtained by using the diverse hybrid power point tracking controllers. The obtained converter current at 320 K by using the VP&O-PSO, and ASHC-fuzzy MPPT controllers are 8.106 A, and 8.806 A respectively.

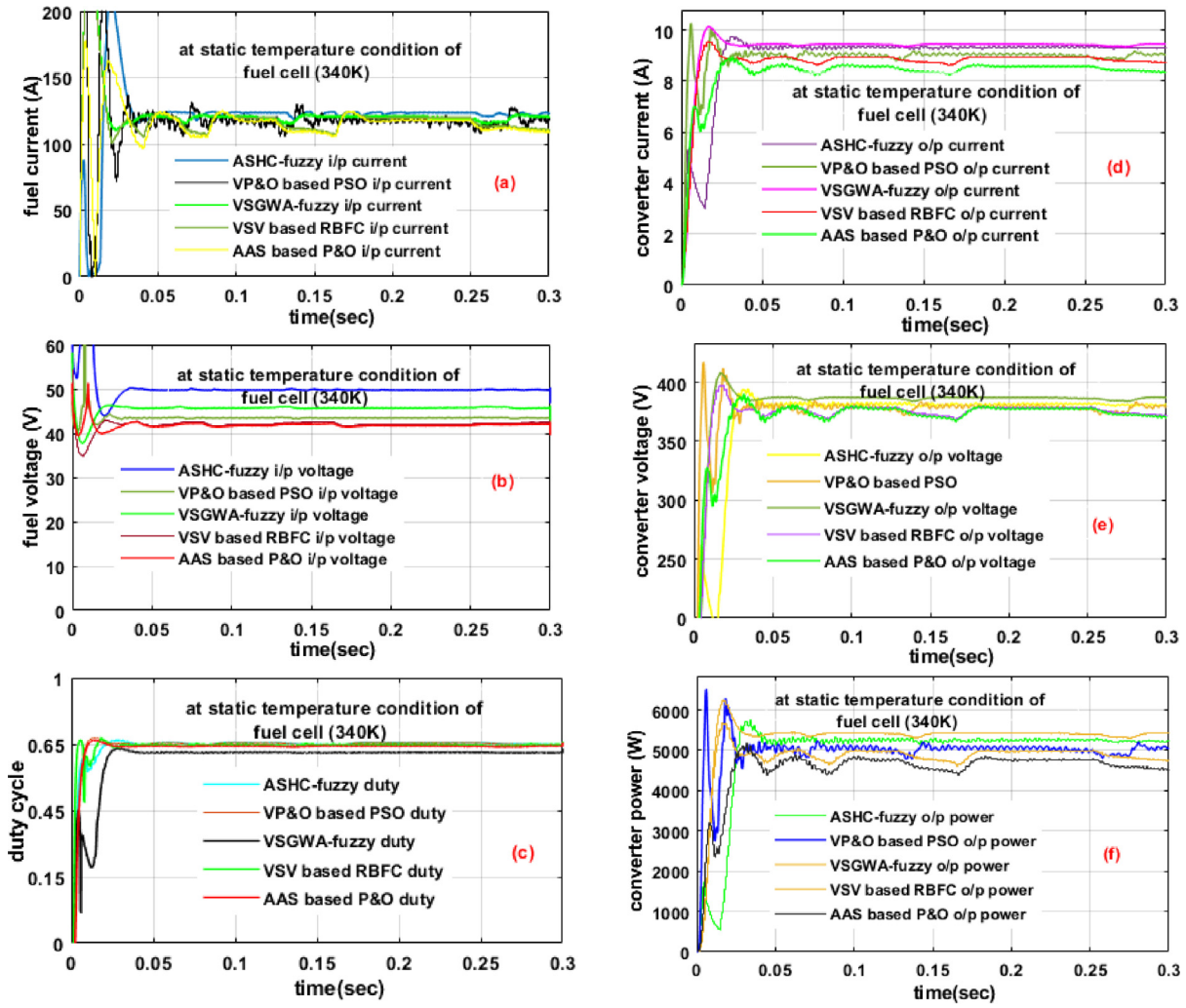

Fig. 14. (a). PEMFC current, (b). PEMFC voltage, (c). Converter duty cycle, (d). Converter current, (e). Converter voltage, and (f). Converter power at a static temperature condition of the fuel stack.

From Fig. 16(d), the converter load current by the use of AAS-based P&O, VSV-based RBFC, ASHC-FLC, VP&O-PSO, and VSGWA-FLC MPPT techniques at 300 K are 7.690 A, 7.969 A, 8.241 A, 8.246 A, and 8.22 A. Here, the converter current is reduced concerning the operating temperature of the fuel cell. The converter output voltage oscillating time, and efficiency by using a GWA-fuzzy controller are 0.142 s, and 98.2% as shown in Fig. 16(e). Also, it is identified that the RBFC technique is easy to understand, and has less implementation cost. But its high oscillations of MPP. At 300 K, the VSGWA-fuzzy, VP&O-PSO, and ASHC-fuzzy logic-based MPPT methods give the maximum peak voltages, and powers which are equal to 41.29 V, 4290.01 W, 41.04 V, 4287.70 W, 40.89 V, and 4283.12 W. Also, the corresponding converter voltages and powers are determined as 512.38 V, 4211.931 W, 507.22 V, 4182.651 W, 505.44 V, and 4165.334 W respectively. The settling time of the converter power at 300 K by using the RBFC technique is 0.095 s which is less than the hybrid GWA-based fuzzy controller. The availability of converter power by the use of different hybrid controllers at dynamic temperature conditions is shown in Fig. 16(f). The detailed performance analysis of hybrid MPPT techniques is given in Table 4.

7. Comprehensive analysis of hybrid MPPT controllers

Here, there are five major parameters are used for the analysis of conventional, soft computing, and metaheuristic MPPT controllers. The selected parameters for the analysis of hybrid MPPT techniques are tracking speed of MPP, oscillations across MPP, the design complexity of the controller, ability to handle fast changes of temperature values, and accuracy of MPP tracking. However, this is not a final comprehensive analysis of various hybrid power point finding controllers because different research scholars compare the different types of parameters for the investigation of MPPT techniques at fast changes of temperature values of the fuel stack. In this work, the authors are annoyed by the comprehensive analysis of hybrid MPPT controllers at fast changes in the operating temperature of fuel cells.

7.1. Tracking speed of MPP

From the literature review, all the fuel cells give nonlinear voltage versus current characteristics at different atmospheric conditions (Sahu et al., 2014). Also, the fuel cell consists of various losses which are ohmic polarization losses, active polarization losses, and concentrated polarization losses. These fuel cell drawbacks are compensated by using the various hybrid MPPT controllers with fast-tracking of MPP. From the simulation results, the conventional AAS-based P&O controller gives less MPP tracking speed when compared to the ASHC-based fuzzy logic controller. At 340 K, the tracking speed of MPP by using the VP&O-based PSO MPPT controllers is 0.14 s Similarly, at 300 K,

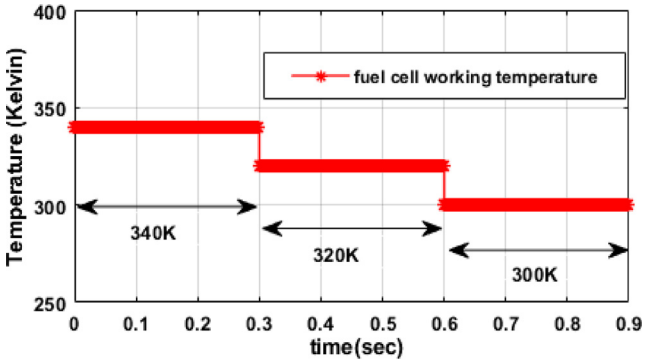

Fig. 15. Dynamic working temperature of the fuel stack.

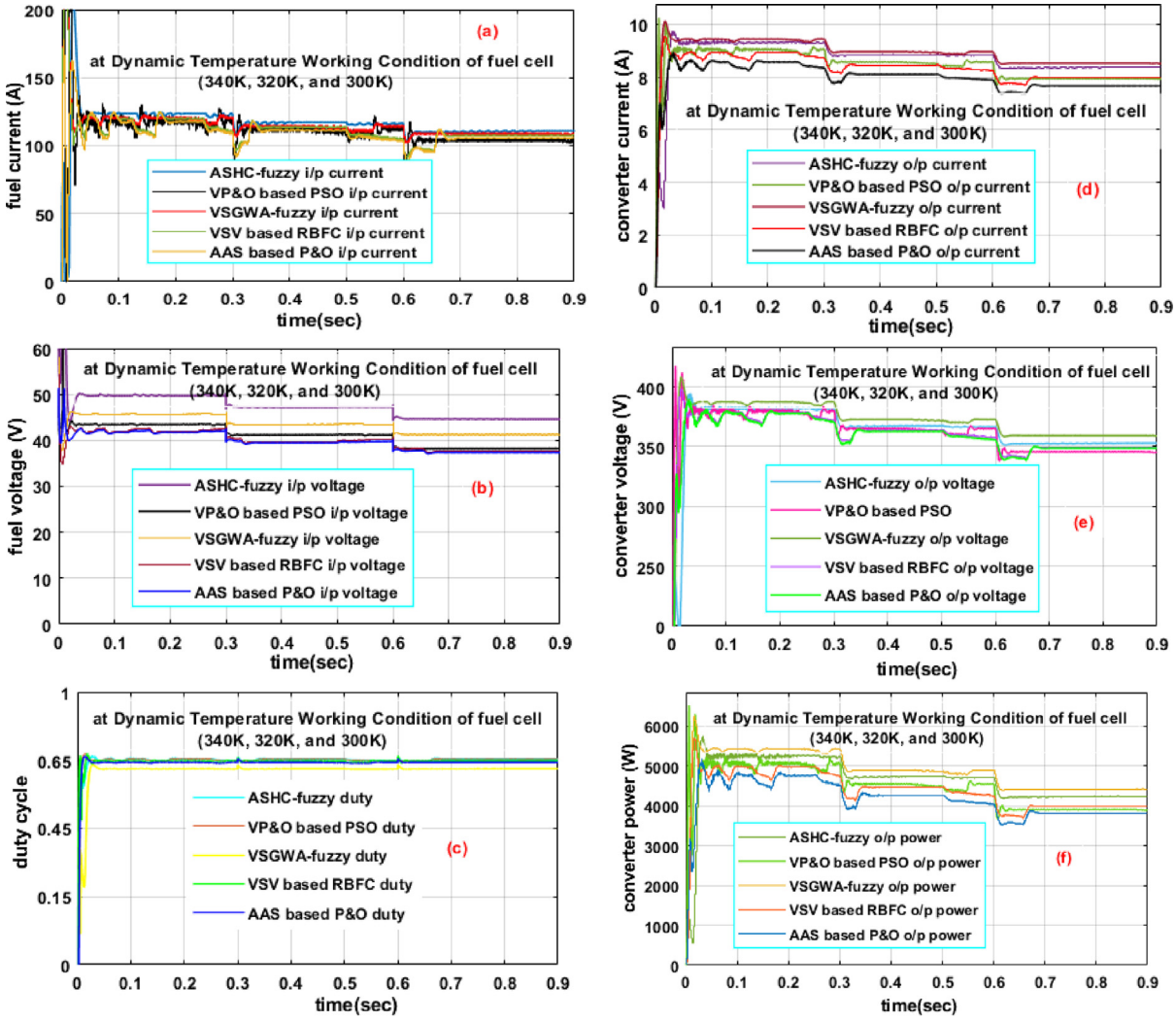

Fig. 16. (a). PEMFC current, (b). PEMFC voltage, (c). Converter duty cycle, (d). Converter current, (e). Converter voltage, and (f). Converter power at a dynamictemperature condition of the fuel stack.

the VSGWA with fuzzy MPPT controller tracking speed of MPP is 0.139 s The other MPPT controllers tracking the speed of MPP are given in Table 4.

7.2. Oscillations across MPP

From Table 1, it is observed that the basic conventional, and swarm intelligence-based power point identifying controllers give more oscillations across MPP. Due to that, the extraction of peak power from the fuel cell stack is very difficult (Park, 2014). Also, the oscillations across MPP give high power flow losses in the proposed system. In this work, from Fig. 14, and 16, the AAS-based P&O, and VSV-based RBFC MPPT techniques give high fluctuated converter output power, and voltage at static as well as dynamic operating temperature conditions of the fuel stack. Similarly, the VSGWA-based MPPT controller gives less oscillations across MPP when compared to the other hybrid metaheuristic MPPT controllers.

Table 4
Analyzing values of proton exchange membrane fuel stack fed conventional converter with various MPPT methods.

Classification of MPPT	Current of input	Voltage of input	Power of input	Current of output	Voltage of output	Power of output	Efficiency	Settling time	Oscillations across MPP	Design Complexity
The working temperature of the fuel cell at 340 K										
AAS-P&O	116.463 A	42.33 V	4929.90 W	8.556 A	556.71 V	4763.269 W	96.62%	0.143 s	High	Moderate
VSV-RBFC	117.732 A	43.48 V	5118.99 W	8.905 A	559.89 V	4985.896 W	97.40%	0.140 s	High	Less
ASHC-fuzzy	120.049 A	44.29 V	5316.98 W	9.236 A	562.80 V	5198.411 W	97.77%	0.128 s	Moderate	High
VP&O-PSO	120.698 A	44.36 V	5353.00 W	9.344 A	563.22 V	5263.069 W	98.32%	0.110 s	Moderate	High
VSGWA-fuzzy	120.622 A	44.38 V	5353.22 W	9.344 A	563.93 V	5269.709 W	98.44%	0.09 s	Less	Moderate
The working temperature of the fuel cell at 320 K										
AAS-P&O	111.086 A	39.88 V	4430.12 W	8.106 A	527.63 V	4277.280 W	96.55%	0.142 s	High	Moderate
VSV-RBFC	112.397 A	40.92 V	4599.31 W	8.475 A	528.43 V	4478.808 W	97.38%	0.138 s	High	Less
ASHC-fuzzy	112.928 A	42.31 V	4777.99 W	8.806 A	529.82 V	4665.707 W	97.65%	0.125 s	Moderate	High
VP&O-PSO	112.817 A	42.59 V	4804.88 W	8.835 A	534.00 V	4717.911 W	98.17%	0.098 s	Moderate	High
VSGWA-fuzzy	109.530 A	43.88 V	4806.2 W	8.772 A	537.99 V	4719.688 W	98.20%	0.091 s	Less	Moderate
Working temperature of the fuel cell at 300 K										
AAS-P&O	103.247 A	38.55 V	3980.19 W	7.690 A	498.99 V	3837.699 W	96.42%	0.139 s	High	Moderate
VSV-RBFC	105.328 A	39.24 V	4133.08 W	7.969 A	500.02 V	3985.115 W	97.25%	0.132 s	High	Less
ASHC-fuzzy	104.747 A	40.89 V	4283.12 W	8.241 A	505.44 V	4165.334 W	97.55%	0.124 s	Moderate	High
VP&O-PSO	104.476 A	41.04 V	4287.70 W	8.246 A	507.22 V	4182.651 W	98.16%	0.095 s	Moderate	High
VSGWA-fuzzy	103.899 A	41.29 V	4290.01 W	8.220 A	512.38 V	4211.931 W	98.18%	0.088 s	Less	Moderate

7.3. Design complexity of MPPT controller

From Section 4, it is identified that the VSV-based RBFC and AAS-based P&O controller's design complexity is very less because these techniques require a very simple setup for tracking the MPP of the fuel stack. Also, the mathematical equations required for the design of conventional controllers are less. The VP&O-PSO, and ASHC-FLC controller's design complexity is very high due to the difficulty of proper membership selection and required a greater number of iterations for the finding of the actual MPP position. The VSGWA-optimized fuzzy logic controller required moderate iterations for the selection of membership functions of the fuzzy system. But it gives maximum power when compared to the conventional controllers.

7.4. Ability to handle the fast change of operating temperature

From the simulation results, the P&O, and RBFC power point tracking controllers give high oscillations across MPP and more settling time of the converter output voltage at fast changes in the operating temperature of the PEM fuel cell. As a result, the conventional, and basic RBFC controllers may not be suitable for the fast changes of working temperature of the fuel cell. From Fig. 16(f), at step changes of working temperature of the fuel cell, the adaptive grey wolf optimized fuzzy system gives very less settling, and rising time of MPP. At 300 K, the settling, and rising time of converter voltage by applying AAS-based P&O, and RBFC controller are 0.139 s, 0.12 s, 0.132 s, and 0.11 s respectively. Similarly, at 340 K, ASHC-FLC gives a less settling time of converter output power when compared to the RBFC controller which is equal to 0.128 s So, the VSGWA-based fuzzy system is having the capability of handling fast changes in the operating temperature of the PEM fuel stack.

7.5. Accuracy of mpp tracking

From Fig. 14(f), and 16 (f), the maximum power extraction from the fuel stack is purely depending on the accuracy of MPP. At 320 K, the extracted fuel cell output powers by using AAS-P&O, VSV-RBFC, and ASHC-fuzzy MPPT techniques are 4430.12 W, 4599.31 W, and 4777.99 W respectively. So, the ASHC-FLC-based power point tracking technique gives high accuracy at static, and fast changes in the operating temperature of the fuel stack when equated with the RBFC controller. Similarly, the obtained fuel cell power by utilizing VSGWA with the fuzzy controller at 300 K is 4290.01 W. Finally, from Table 4, the variable step grey wolf controller optimized fuzzy controller is giving high accuracy in MPP tracking at different step changes of temperature conditions.

8. Conclusion

From the detailed literature study, the proton exchange membrane fuel stack system is selected for the analysis of different MPPT techniques at various operating temperature conditions of the fuel stack. The merits of PEMFC are high power density, low volume, high power conversion efficiency, fast startup, and less weight. After that, the hybrid AAS-based P&O, VSV-based RBFC, ASHC-fuzzy, VP&O-PSO, and VSGWA-fuzzy MPPT techniques are studied for the PEMFC system at static and dynamic operating temperature conditions. The selected hybrid controller's comparative analysis has been done in terms of tracking speed of MPP, oscillations across MPP, design complexity of controller, ability to handle fast changes of temperature values, and accuracy of MPP tracking. From the simulative study, it is observed that the variable step grey wolf algorithm optimized fuzzy logic controller is giving a superior performance at static as well as dynamic operating temperature conditions of the fuel stack. Here, the conventional non-isolated boost converter is used for enhancing the output voltage of the fuel stack. The merits of the conventional converter are ease of design, less implementation cost, and high flexibility.

CRediT authorship contribution statement

Shaik Rafikiran: Conceptualization, Methodology, Software, Data curation, Writing – original draft. **G. Devadasu:** Data curation, Writing – original draft. **C.H. Hussaian Basha:** Writing – original draft, Software, Data curation. **Pretty Mary Tom:** Visualization, Investigation. **Prashanth V.:** Writing – reviewing and editing. **Dhanamjayulu C.:** Supervision, Investigation Project admiration, Conceptualization. **Abhishek Kumbhar:** Validation, Writing – reviewing and editing. **S.M. Muyeen:** Supervision, Project admiration, Funding, Conceptualization.

Declaration of competing interest

We declare that this manuscript is original, has not been published before and is not currently being considered for publication elsewhere. We do not have any conflict of interest and will be grateful if you consider it.

Data availability

No data was used for the research described in the article.

Acknowledgments

Open Access funding provided by the Qatar National Library.

References

Ahmad, Shahbaz, et al., 2022. An overview of proton exchange membranes for fuel cells: Materials and manufacturing. Int. J. Hydrogen Energy.
Alaraj, Muhannad, Radenkovic, Miloje, Park, Jae-Do, 2017. Intelligent energy harvesting scheme for microbial fuel cells: Maximum power point tracking and voltage overshoot avoidance. J. Power Sources 342, 726–732.
Ali, M.S., et al., 2014. An overview of power electronics applications in fuel cell systems: DC and AC converters. Sci. World J. 2014.
Ali, Ziad M., et al., 2023. A new maximum power point tracking method for PEM fuel cell power system based on ANFIS with modified manta ray foraging algorithm. Control Eng. Pract. 134, 105481.
Alias, M.S., et al., 2020. Active direct methanol fuel cell: An overview. Int. J. Hydrogen Energy 45 (38), 19620–19641.
Awin, Yussef, Dukhan, Nihad, 2019. Experimental performance assessment of metal-foam flow fields for proton exchange membrane fuel cells. Appl. Energy 252, 113458.
Azri, Maaspaliza, et al., 2017. Fuel cell emulator with MPPT technique and boost converter. Int. J. Power Electron. Drive Syst. 8 (4), 1852.
Badoud, Abd Essalam, Mekhilef, Saad, Ould Bouamama, Belkacem, 2021. A novel hybrid MPPT controller based on bond graph and fuzzy logic in proton exchange membrane fuel cell system: Experimental validation. Arab. J. Sci. Eng. 1–20.
Bargal Mohamed, HS., et al., 2020. Liquid cooling techniques in proton exchange membrane fuel cell stacks: A detailed survey. Alex. Eng. J. 59 (2), 635–655.
Basha, C.H. Hussaian, Rani, C., 2022. A new single switch DC-DC converter for PEM fuel cell-based electric vehicle system with an improved beta-fuzzy logic MPPT controller. Soft Comput. 26 (13), 6021–6040.
Basha, CH Hussaian, et al., 2022. Simulative design and performance analysis of hybrid optimization technique for PEM fuel cell stack based EV application. Mater. Today Proc. 52, 290–295.
Basha, C.H. Hussaian, et al., 2023. Design of GWO based fuzzy MPPT controller for fuel cell fed EV application with high voltage gain DC-DC converter. Mater. Today Proc..
Bigdeli, Nooshin, 2015. Optimal management of hybrid PV/fuel cell/battery power system: A comparison of optimal hybrid approaches. Renew. Sustain. Energy Rev. 42, 377–393.
Chen, Pi-Yun, et al., 2017. A novel variable step size fractional order incremental conductance algorithm to maximize power tracking of fuel cells. Appl. Math. Model. 45, 1067–1075.
Deng, Shipei, Li, Yinshi, 2022. A porous-rib flow field for performance enhancement in proton exchange membrane fuel cells. Energy Convers. Manage. 263, 115707.
El Otmani, F., et al., 2020. MPPT based sliding mode control for fuel cell connected grid system. IFAC-PapersOnLine 53 (2), 13322–13327.
Elsayad, Nour, Moradisizkoohi, Hadi, Mohammed, Osama A., 2019. A new single-switch structure of a DC–DC converter with wide conversion ratio for fuel cell vehicles: Analysis and development. IEEE J. Emerg. Sel. Top. Power Electron. 8 (3), 2785–2800.
Ferguson, Suzanne, Tarrant, Anthony, 2021. Molten carbonate fuel cells for 90% post combustion CO2 capture from a new build CCGT. Front. Energy Res. 9, 668431.
Fuzato, Guilherme HF., et al., 2016. Voltage gain analysis of the interleaved boost with voltage multiplier converter used as electronic interface for fuel cells systems. IET Power Electron. 9 (9), 1842–1851.
Ge, Zheng, et al., 2015. Energy extraction from a large-scale microbial fuel cell system treating municipal wastewater. J. Power Sources 297, 260–264.
Ghoshal, Snehashis, et al., 2022. Performance analysis of PV-fuel cell hybrid system in small scale DC system. In: 2022 Second International Conference on Advances in Electrical, Computing, Communication and Sustainable Technologies. ICAECT, IEEE.
Girirajan, Balasubramanian, et al., 2022. High gain converter with improved radial basis function network for fuel cell integrated electric vehicles. World Electr. Veh. J. 13 (2), 31.
Gong, Chengyuan, Luo, Xiaobing, Tu, Zhengkai, 2022. Performance evaluation of a solid oxide fuel cell multi-stack combined heat and power system with two power distribution strategies. Energy Convers. Manage. 254, 115302.
Gopal, S. Madan, Meenendranath Reddy, K., 2023. Design and control of high voltage gain interleaved boost converter for fuel cell based electric vehicle applications. J. Electron. Comput. Netw. Appl. Math. (JECNAM) (ISSN: 2799-1156) 3 (02), 9–24.
Goudarzian, Alireza, Khosravi, Adel, Ali Raeisi, Heidar, 2022. Modeling, design and control of a modified flyback converter with ability of right-half-plane zero alleviation in continuous conduction mode. Eng. Sci. Technol. Int. J. 26, 101007.
Grumm, Florian, et al., 2020. Short circuit characteristics of PEM fuel cells for grid integration applications. Electronics 9 (4), 602.
Gugulothu, Ramesh, Nagu, Bhookya, Pullaguram, Deepak, 2022. A computationally efficient jaya optimization for fuel cell maximum power tracking. Energy Sour. Part A: Recov. Util. Environ. Eff. 44 (1), 1541–1565.
Guo, Xiaokai, Sepanta, Mehdi, 2021. Evaluation of a new combined energy system performance to produce electricity and hydrogen with energy storage option. Energy Rep. 7, 1697–1711.
Hai, Tao, et al., 2023. Performance improvement of PEM fuel cell power system using fuzzy logic controller-based MPPT technique to extract the maximum power under various conditions. Int. J. Hydrogen Energy 48 (11), 4430–4445.
Hussaian Basha, C.H., Rani, C., 2020. Performance analysis of MPPT techniques for dynamic irradiation condition of solar PV. Int. J. Fuzzy Syst. 22 (8), 2577–2598.
Hussaian Basha, C.H., et al., 2022. Design of adaptive VSS-P & O-based PSO controller for PV-based electric vehicle application with step-up boost converter. In: Pattern Recognition and Data Analysis with Applications. Springer Nature Singapore, Singapore, pp. 803–817.
Hwu, Kuo-Ing, Jiang, Wen-Zhuang, Chien, J.Y., 2016. Isolated high voltage-boosting converter derived from forward converter. Int. J. Circuit Theory Appl. 44 (2), 280–304.
Izdebski, Waldemar, Kosiorek, Katarzyna, 2023. Analysis and evaluation of the possibility of electricity production from small photovoltaic installations in Poland. Energies 16 (2), 944.
Jayalakshmi, N.S., Gaonkar, D.N., Bhat Nempu, Pramod, 2016. Power control of PV/fuel cell/supercapacitor hybrid system for stand-alone applications. Int. J. Renew. Energy Res. (IJRER) 6 (2), 672–679.
Jianfeng, Lv., et al., 2023. Diagnosis of PEM fuel cell system based on electrochemical impedance spectroscopy and deep learning method. IEEE Trans. Ind. Electron..
Kanouni, Badreddine, Mekhilef, Saad, 2022a. A multi-objective model predictive current control with two-step horizon for double-stage grid-connected inverter PEMFC system. Int. J. Hydrogen Energy 47 (4), 2685–2707.
Kanouni, Badreddine, Mekhilef, Saad, 2022b. A SMC-based MPPT controller for proton exchange membrane fuel cell system. In: 2022 19th International Multi-Conference on Systems, Signals & Devices. SSD, IEEE.
Khan, Mohammad Junaid, Mathew, Lini, 2019. Fuzzy logic controller-based MPPT for hybrid photo-voltaic/wind/fuel cell power system. Neural Comput. Appl. 31, 6331–6344.
Kiran., Shaik Rafi, et al., 2022. A new design of single switch DC-DC converter for PEM fuel cell based EV system with variable step size RBFN controller. Sādhanā 47 (3), 128.
Kiran, Shaik Rafi, et al., 2022. Reduced simulative performance analysis of variable step size ANN based MPPT techniques for partially shaded solar PV systems. IEEE Access 10, 48875–48889.
Kolli, Abdelfatah, et al., 2015. A review on DC/DC converter architectures for power fuel cell applications. Energy Convers. Manage. 105, 716–730.
Kurnia, Jundika C., et al., 2021. Progress on open cathode proton exchange membrane fuel cell: Performance, designs, challenges and future directions. Appl. Energy 283, 116359.
Lu, Chia-Lien, et al., 2019. High-performance and low-leakage phosphoric acid fuel cell with synergic composite membrane stacking of micro glass microfiber and nano PTFE. Renew. Energy 134, 982–988.
Musumeci, S., Di Mauro, S., 2017. Low voltage single fuel cell interface by push-pull converter: A case of study. In: 2017 6th International Conference on Clean Electrical Power. ICCEP, IEEE.
Naik, M., Venkatesh, Samuel, Paulson, 2016. Analysis of ripple current, power losses and high efficiency of DC–DC converters for fuel cell power generating systems. Renew. Sustain. Energy Rev. 59, 1080–1088.
Nayak, Anish K., Ganguli, Babu, Ajayan, Pulickel M., 2023. Advances in electric two-wheeler technologies. Energy Rep. 9, 3508–3530.
Nureddin, Abdulbaset Abdulhamed Mohamed, Rahebi, Javad, Ab-BelKhair, Adel, 2020. Power management controller for microgrid integration of hybrid PV/fuel cell system based on artificial deep neural network. Int. J. Photoenergy 2020, 1–21.
Park, Heesung, 2014. Numerical assessment of liquid cooling system for power electronics in fuel cell electric vehicles. Int. J. Heat Mass Transfer 73, 511–520.
Pasternak, Antonella, Bresser, Charis, 2022. Developing hierarchical RBF neural network for model identification of SOFCs using a developed coronavirus herd immunity algorithm. J. Smart Syst. Stable Energy 1 (4), 319–332.
Promsen, Mungmuang, et al., 2022. Metallic PCM-integrated solid oxide fuel cell stack for operating range extension. Energy Convers. Manage. 255, 115309.
Rafikiran, Shaik, et al., 2023. Design of high voltage gain converter for fuel cell based EV application with hybrid optimization MPPT controller. Mater. Today Proc..

Rajesh, K., 2023. Radial basis function neural network MPPT controller-based microgrid for hybrid stand-alone energy system used for irrigation. Circuit World 49 (2), 251–266.
Rajesh, P., Shajin, Francis H., Umasankar, L., 2021. A novel control scheme for PV/WT/FC/battery to power quality enhancement in micro grid system: A hybrid technique. Energy Sour. Part A: Recov. Util. Environ. Eff. 1–17.
Rana, K.P.S., et al., 2019. A novel dPdI feedback based control scheme using GWO tuned PID controller for efficient MPPT of PEM fuel cell. ISA Trans. 93, 312–324.
Rasheed, Muhammad Babar, R-Moreno, María D., Gamage, Kelum.AA., 2022. Artificial intelligence-enabled probabilistic load demand scheduling with dynamic pricing involving renewable resource. Energy Rep. 8, 14034–14047.
Reddy, K., Jyotheeswara, Sudhakar, N.J.I.A., 2018. High voltage gain interleaved boost converter with neural network based MPPT controller for fuel cell based electric vehicle applications. Ieee Access 6, 3899–3908.
Reddy, B. Raja Sekhar, Veera Reddy, VC., Vijaya Kumar, M., 2023. Modelling and analysis of DC-DC converters with AI based MPP tracking approaches for grid-tied PV-fuel cell system. Electr. Power Syst. Res. 216, 109053.
Rezk, Hegazy, 2016. Performance of incremental resistance MPPT based proton exchange membrane fuel cell power system. In: 2016 Eighteenth International Middle East Power Systems Conference. MEPCON, IEEE.
Rezk, Hegazy, Fathy, Ahmed, 2020. Performance improvement of PEM fuel cell using variable step-size incremental resistance MPPT technique. Sustainability 12 (14), 5601.
Safarishaal, Masoud, Sarvi, Mohammad, 2023. New hybrid maximum power point tracking methods for fuel cell using artificial intelligent. AIP Adv. 13 (4), 045207, 44.
Sahu, Ishwar Prasad, et al., 2014. Performance study of PEM fuel cell under different loading conditions. Energy Procedia 54, 468–478.
Silaa, Mohammed Yousri, et al., 2020. Design and implementation of high order sliding mode control for PEMFC power system. Energies 13 (17), 4317.
Somaiah, Boddu, Agarwal, Vivek, 2016. Distributed maximum power extraction from fuel cell stack arrays using dedicated power converters in series and parallel configuration. IEEE Trans. Energy Convers. 31 (4), 1442–1451.
Souissi, Ahmed, 2021. Adaptive sliding mode control of a PEM fuel cell system based on the super twisting algorithm. Energy Rep. 7, 3390–3399.
Srinivasan, Suresh, et al., 2021. Neural network based MPPT control with reconfigured quadratic boost converter for fuel cell application. Int. J. Hydrogen Energy 46 (9), 6709–6719.
Su, Yulong, et al., 2023. Rigdelet neural networks-based maximum power point tracking for a PEMFC connected to the network with interleaved boost converter optimized by improved Satin Bowerbird optimization. Energy Rep. 9, 4960–4970.
Subhransu, Padhee, Chandra Pati, Umesh, Mahapatra, Kamalakanta, 2016. Comparative analysis of DC-DC converter topologies for fuel cell based application. In: 2016 IEEE 1st International Conference on Power Electronics, Intelligent Control and Energy Systems. ICPEICES, IEEE.
Szczśniak, Arkadiusz, et al., 2020. Dynamic model of a molten carbonate fuel cell 1 kW stack. Energy 200, 117442.
Tytelmaier, Kostiantyn, et al., 2016. A review of non-isolated bidirectional dc-dc converters for energy storage systems. In: 2016 II International Young Scientists Forum on Applied Physics and Engineering. YSF, IEEE.
Wang, Hanqing, Gaillard, Arnaud, Hissel, Daniel, 2019. A review of DC/DC converter-based electrochemical impedance spectroscopy for fuel cell electric vehicles. Renew. Energy 141, 124–138.
Wei, Yuqi, Luo, Quanming, Mantooth, Alan, 2020. A hybrid half-bridge LLC resonant converter and phase shifted full-bridge converter for high step-up application. In: 2020 IEEE Workshop on Wide Bandgap Power Devices and Applications in Asia. WiPDA Asia, IEEE.
Wilailak, Supaporn, et al., 2021. Thermo-economic analysis of phosphoric acid fuel-cell (PAFC) integrated with organic ranking cycle (ORC). Energy 220, 119744.
Wu, Qunfang, et al., 2017. Implementation of an active-clamped current-fed push–pull converter employing parallel-inductor to extend ZVS range for fuel cell application. IEEE Trans. Ind. Electron. 64 (10), 7919–7929.
Yahia, Foughali, et al., 2022. Predicting PEMFC maximum power point using an artificial neural network. In: 2022 2nd International Conference on Advanced Electrical Engineering. ICAEE, IEEE.
Yu, Xin, et al., 2021. Numerical investigation of a new combined energy cycle based on miller cycle, organic rankine cycle, stirling engine and alkaline fuel cell. Energy Rep. 7, 5406–5419.
Yu, Xianxian, et al., 2022. Effects of anode flow channel on performance of air-cooled proton exchange membrane fuel cell. Energy Rep. 8, 4443–4452.
Yuan, Zhi, et al., 2020. Parameter identification of PEMFC based on convolutional neural network optimized by balanced deer hunting optimization algorithm. Energy Rep. 6, 1572–1580.
Zheng, Jianqin, et al., 2023. A hybrid framework for forecasting power generation of multiple renewable energy sources. Renew. Sustain. Energy Rev. 172, 113046.